Kinetic data for modeling the dynamics of the enzymes involved in animal fatty acid synthesis

Chilperic Armel Foko Kuate, Oliver Ebenhöh, Barbara M. Bakker, Adélaïde Raguin

Article - Version of Record

Bioscience Reports (2023) **43** BSR20222496
https://doi.org/10.1042/BSR20222496

PORTLAND PRESS

Review Article

Kinetic data for modeling the dynamics of the enzymes involved in animal fatty acid synthesis

Chilperic Armel Foko Kuate[1,2,3], Oliver Ebenhöh[1,3], Barbara M. Bakker[4] and Adélaïde Raguin[2,3]

[1]Institute for Quantitative and Theoretical Biology, Biology department, Heinrich Heine University, Düsseldorf, Germany; [2]Institute for Computational Cell Biology, Computer Science department, Heinrich Heine University, Düsseldorf, Germany; [3]Cluster of Excellence on Plant Sciences (CEPLAS), Heinrich Heine University, Düsseldorf, Germany ; [4]Institute for Systems Medicine of Metabolism and Signaling, Pediatrics department, University of Groningen, University Medical Center Groningen, Groningen, The Netherlands

Correspondence: Adélaïde Raguin (adelaide.raguin@hhu.de)

The synthesis and modification of fatty acids (FAs) from carbohydrates are paramount for the production of lipids. Simultaneously, lipids are pivotal energy storage in human health. They are associated with various metabolic diseases and their production pathways are for instance candidate therapeutic targets for cancer treatments. The fatty acid *de novo* synthesis (FADNS) occurs in the cytoplasm, while the microsomal modification of fatty acids (MMFA) happens at the surface of the endoplasmic reticulum (ER). The kinetics and regulation of these complex processes involve several enzymes. In mammals, the main ones are the acetyl-CoA carboxylase (ACC), the fatty acid synthase (FAS), the very-long-chain fatty acid elongases (ELOVL 1–7), and the desaturases (delta family). Their mechanisms and expression in different organs have been studied for more than 50 years. However, modeling them in the context of complex metabolic pathways is still a challenge. Distinct modeling approaches can be implemented. Here, we focus on dynamic modeling using ordinary differential equations (ODEs) based on kinetic rate laws. This requires a combination of knowledge on the enzymatic mechanisms and their kinetics, as well as the interactions between the metabolites, and between enzymes and metabolites. In the present review, after recalling the modeling framework, we support the development of such a mathematical approach by reviewing the available kinetic information of the enzymes involved.

Introduction

Fatty acids (FAs) are of utmost biological importance for living systems. Their synthesis pathway varies among plants, bacteria, and animals [1,2]. They are building blocks for lipids and the primary form of energy storage. Besides their energy-related role, FAs are the main constituents of cellular and organellar membranes, precursors for several signaling pathways, and play an anti-inflammatory role [3,4]. In animals, recent investigations suggest their importance as therapeutic candidates for various disorders. They are involved in cancer [5,6], nonalcoholic fatty liver disease [7], type II diabetes [8], obesity, and inherited metabolic conditions such as fatty acid oxidation disorders [9,10]. Considering the central role of FAs for human medical and nutritional applications, we focus on animals with particular attention on mammals. Mathematical and computational modeling has become increasingly popular and successful in the investigation of pathway dynamics, as it allows to decipher complex systems, and interpret counter-intuitive observations [11]. It includes both static methods (e.g., genome-scale flux balance analysis, atom mapping, and network topology analysis) and dynamic ones (e.g., stochastic or deterministic modeling, and stable isotope tracers) [12–17].

The present review is addressed to mathematical system biologists who aim to model the dynamics of animal fatty acid synthesis using ordinary differential equation (ODE) models based on kinetic rate laws, a typical deterministic approach. The kinetic rate laws and associated parameters for the FA β-oxidation are largely available in the literature [18–25] as demonstrated by the model of van Eunen and coworkers [24].

Received: 05 December 2022
Revised: 06 April 2023
Accepted: 03 May 2023

Accepted Manuscript online: 03 May 2023
Version of Record published: 19 July 2023

Bioscience Reports (2023) **43** BSR20222496
https://doi.org/10.1042/BSR20222496

Yet, analogous information in the case of fatty acid synthesis is scarce. We, therefore, choose to focus on the latter and review the kinetic features of the key enzymes involved in the main pathways of animal fatty acid synthesis (mainly mammals). This includes fatty acid *de novo* synthesis (FADNS), and microsomal modifications (elongation and desaturation) for both endogenous and exogenous FAs. Noticeably, we do not report on the mitochondrial fatty acid synthesis, and we neglect enzymes and transporters that have only a secondary impact on the fatty acid synthesis, e.g., the malonyl-CoA decarboxylase, the acyl-CoA, and the fatty acid-binding proteins. The first section smoothly introduces a nonspecialist reader to the modeling framework, and motivates the latter in comparison with other methods. Then, we individually present the enzymes involved and summarize their kinetic information necessary for modeling. In the Discussion and Conclusions section, we highlight potential new research directions that still require further investigations. In the Supplementary Material section, we provide tables with kinetic parameters and the corresponding rate laws.

Nomenclature

Two distinct nomenclatures of FAs are spread in the field, i.e., delta and omega. Throughout the paper, we use the latter one. Then, *X:Yn-Z* stands for a FA with *X* carbon atoms and *Y* double bonds (*X:0* describes a saturated FA), and *Z* is the position of the first double bond counted from the methyl end. Because of the way they are introduced, double bonds appear with a spacing of three carbon atoms. Most naturally occurring FAs have an even number of carbon atoms.

Enzyme kinetic modeling using rate laws

The framework

Metabolism is the set of chemical reactions that allows organisms to perform their biological functions. As it involves thousands of enzymes, it is divided into pathways, for instance, defined as the ensemble of reactions leading to the production or the consumption of particular compounds. Pathways can be studied from a static or a dynamic point of view, which is chosen depending on the size of the pathway, the questions to be addressed, the pre-existing information, and the assumptions. Static modeling, such as stoichiometric models and constraint-based models, allows studying the distinct metabolic routes and the associated fluxes at the steady states [12,26]. They are particularly relevant for large-scale models (e.g., genome-scale) that involve up to thousands of reactions and metabolites. However, if one is interested in tracking metabolites change over time, dynamical models are required. Furthermore, access to the concentration of the system's metabolites over time allows to discriminate optimal fluxes predicted by static models that may pass through biologically unrealistic transient states. Among dynamic models, one could differentiate between deterministic and stochastic ones. The latter specifically allow to study systems made of a small number of entities, their fluctuations, and to represent *in silico* large and complex substrates for which kinetic rate laws cannot be derived (e.g., glycogen). In the present review, we focus on the FA biosynthesis pathway and provide biochemical information to construct models simulating its dynamics based on kinetic rate laws. Thereby, one can study metabolic pathways both qualitatively and quantitatively. Kinetic rate laws define the velocity at which a chemical reaction occurs while highlighting the underlying mechanism, the contribution of each element participating in the reaction, and their interactions [27,28].

The rate of change over time of individual chemical entities (noted M_i) is expressed as the sum and difference of rate law terms (noted v_j), weighted by their stoichiometric coefficients (noted α_{ij}), following (eqn 1.1):

$$\frac{dM_i}{dt} = \sum_j \alpha_{ij} v_j \tag{1.1}$$

A good overview of some simple and commonly used kinetic rate laws has been published by Saa and Nielsen [29], as well as Kim et al. [12]. The closer a reaction is to the equilibrium, the least details are needed to model it. Kinetic rate laws require parameters that can be estimated from experimental data using methods such as Lineweaver-Burk plots [30–32], Hanes-Woolf plots [33], and nonlinear regressions [34]. Still, when missing kinetic parameters, the typical approach consists in either using those from a related organism, or implementing simplistic rate laws such as mass-action kinetics or its generalization. Although these types of rate laws are easy to analyze, they have the disadvantage of not capturing substrate saturation [35]. To circumvent this limitation, more complex kinetics can be used, such as Michaelis–Menten [36], multisubstrate (sequential or ping-pong) [27], 'convenience' [35] or 'universal' [37] kinetics. They account for the order of addition of the substrates, the order of formation of the products, the different types of inhibition, the activations, the competitions, etc. Aside from these strengths, the potentially large number of parameters is usually an obstacle for further analysis. Besides, the King and Altman method is a generic

approach to derive kinetic rate laws, step-by-step, from the underlying specific enzymatic mechanism [38–40]. It allows determining the kinetic rate laws of complex mechanisms involving one or more reactants, products, inhibitors, etc. The steps of the method have been fully described by Cleland et al. [27] and Ulusu et al. [41]. Simpler kinetics such as Michaelis–Menten can also be retrieved by this means. In addition, the Haldane relationship can be used to relate the kinetic parameters and the thermodynamics of the reaction via the equilibrium constant.

Generally, the mathematical representation of the dynamics of the pathway leads to large systems of nonlinear differential equations that are difficult or impossible to solve and interpret analytically. Therefore, dedicated software tools have been developed to solve them numerically. Among others, we can mention Modelbase [42], COPASI [43], PySCeS [44], and Berkeley Madonna [45].

Aims of the method

Kinetic models can help testing hypotheses, designing and assisting experiments, discriminating between possible regulatory mechanisms, identifying drug targets, and make sense of genomic, proteomic, and metabolic data [29,46–48]. They allow predicting how the system responds to perturbations, or identify the existence of rescuing pathway routes, for example, toward understanding disease phenotypes. They also can be used to predict the time course of metabolite concentrations and fluxes, for instance, toward optimizing the latter. For illustration, we report here a typical example where theory-derived hypotheses have been verified experimentally and led to major progress in understanding the associated metabolic pathway. It is known that hypoglycemia observed in medium chain acyl-CoA dehydrogenase deficiencies is the result of the inability of β-oxidation to deal with substrate influx, because one of the first enzymes involved in this cyclic pathway is defective. Remarkably, using a detailed kinetic model, based on a bottom-up approach and a set of mice experiments, Martines et al. [10] have been able to predict that intermediate metabolites accumulate within the pathway, causing the reverse reactions to be more thermodynamically favorable than the forward ones. Using metabolic control analysis, they also showed that medium-chain ketoacyl-CoA thiolase (MCKAT) can restore the pathway fluxes, revealing its potential for being a drug target. As an incentive, we additionally present two specific cases of experimental observations that would typically benefit from a complementary kinetic modeling investigation. First, experimental results by Santos and Schulze [49], and de Cedrón and de Molina [50], showed that targeting acetyl-CoA carboxylase (ACC) and fatty acid synthase (FAS), or adopting appropriate diet habits, holds the potential to reduce tumor growth, since long-chain-saturated fatty acids (LCSFAs) are considered as a fuel for tumor proliferation [51,52]. Beyond this qualitative observation, the quantitative details of these therapeutic approaches are not specified, nor their consequences on the whole lipid metabolism. A kinetic model could help to quantitatively characterize the respective contribution of each enzyme to the overall LCSFAs *de novo* production, thereby unveiling their potential as drug target. One should note that, although Menendez and Lupu [52] showed that FADNS is more pronounced in tumor cells, tumor proliferation is a complex process that involves several factors (see the review by Fhu and Ali [53]). Second, in FA metabolic disorders, such as obesity and type 2 diabetes, Lelliott and Vidal-Puig [54] observed lipotoxicity caused by an imbalance between *de novo* lipogenesis and FA oxidation. To counteract this effect, the authors suggested to both decrease the fat deposition in the white adipose tissues, and to increase the FA oxidation capacity of oxidative tissues. To test this hypothesis, one could develop a lipid metabolism model that includes both lipogenic and oxidative tissues, as well as, all biochemical reactions relating to FA metabolism and their hormonal regulation, at the whole body level. Furthermore, the model should allow to quantify the FA fluxes and concentrations in each tissue in a time-dependent manner. To fulfill these requirements, and ensure that the theoretical parameter values resulting from the model do not correspond to unrealistic biology, e.g., thermodynamically unfeasible, a kinetic model appears most appropriate.

FADNS

The FADNS, also known as the endogenous synthesis of FAs, produces LCSFAs from acetyl-CoA in presence of ATP, bicarbonate (HCO_3^-), and NADPH. The process can be divided into two parts: (i) the synthesis of malonyl-CoA from acetyl-CoA by the biotin enzyme ACC, and (ii) the step-wise elongation of the acyl-CoA chain by the multicomplex enzyme FAS. The main resulting product is palmitic acid (16:0), together with some myristic (14:0) and stearic (18:0) acids, and very low amounts of lauric (12:0) and arachidic (20:0) acids [55–57]. Below, we provide a brief introduction to the biochemistry of each enzyme. For further details, the reader is referred to [58,59] for ACC and [1,2,60] for FAS. In addition, for the reader to construct their models, we tabulated the kinetic rate laws associated to the enzymes (see Table 1). To keep our tables short, we focus on the simplest kinetic laws. For the more complex ones, we refer the reader to the original articles discussed in the text. We also gathered the associated kinetic parameters (see Tables 2 and 3). Several blanks appear in both tables, highlighting some of the gaps in the data availability.

Bioscience Reports (2023) **43** BSR20222496
https://doi.org/10.1042/BSR20222496

Table 1 Kinetic rate laws corresponding to the parameters reported in Tables 2, 3, and 6–8

Enzyme	Rate law	Formula	Parameters	Reference
ACC	Competitive inhibition and activation	$V_{max} \times S/(K_m(1 + I/K_i) + S(1 + K_a/A))$	Table 2	[68]
ACC ELOVL Δ-9, Δ-5, Δ-6	Michaelis–Menten kinetics	$k_{cat} \times E_0 \times S/(K_m + S) = V_{max} \times S/(K_m + S)$	Tables 2, 3, and 6–8	[66,89,92,108–110, 122–124,126–128,134]
FAS		$k_{cat} \times E_0/(1 + K_{M_{M\,al}}/M\,al(1 + Acet/K_{I_{Acet}}) + K_{M_{A\,cet}}/Acet$ (1+M $al/K_{I_{M\,al}}$) + $K_{M_{NADPH}}/NADPH$)	Table 3	[34]

Although some of the kinetic features discussed here are not from mammals, they can still be used as a starting point for modeling. They typically share a similar enzymatic mechanism, as well as high amino acid sequence identity. For instance, chicken and rat FAS sequences are 63% and 79% identical to that of human, respectively [61]. Besides, among mammals, it is observed that murine FAS sequence is 81%, 78%, and 94% identical to that of human, pig, and rat, respectively [33].

ACC

ACC is a key enzyme for lipid homeostasis [62,63]. To date, two isoforms of ACC are known (i.e., ACC1 and ACC2). They are encoded by two distinct genes that share 80% of similarity when comparing their amino acid sequences. One of the major differences between the two isoforms resides in their N-terminal amino acid sequences [64]. For ACC2, the latter starts with hydrophobic residues that are responsible for its membrane-bound properties and its location at the surface of the mitochondrial outer membrane [64,65]. Opposite, ACC1 is a soluble cytosolic enzyme (see Figure 1). Despite these differences, ACC1 and ACC2 share a similar mechanism, and noticeably, they are reported with comparable kinetic parameter values (see Table 2) [66–68]. More precisely, we can remark that in the study by Cheng et al. [66], for human ACC1 and ACC2, the k_{cat} values measured are almost indistinguishable (when considering the standard errors) and the K_m values show very similar tendencies for the three substrates considered. In the same study, the authors observed comparable values for ACC2 in rat. In addition to show distinct location in the cell, ACC1 and ACC2 have different tissue-specific expression. The ACC1 isoform, which is found in all tissues, is particularly highly expressed in lipogenic tissues such as the liver, adipose tissues, and mammary glands. The second isoform, ACC2, is mostly present in oxidative tissues such as the heart and the skeletal muscles. It is also expressed, to a lesser extent, in lipogenic tissues [69–71]. In the respective tissues, the malonyl-CoA produced by ACC1 is utilized for elongation in FADNS, while the one from ACC2 also inhibits the carnitine palmitoyl transferase 1 and thereby the β-oxidation [65,72].

Both ACC isoforms synthesize malonyl-CoA from acetyl-CoA in three steps. First, the ACC is carboxylated, using HCO_3^- as carbon donor in presence of ATP. Second, the carboxyl group is transferred between the catalytic sites of the enzyme. Third, the carboxyl group reacts with acetyl-CoA to form malonyl-CoA [66]. Citrate, exported from mitochondria, is converted in cytosolic acetyl-CoA, which is further converted into malonyl-CoA by ACC1 and ACC2 enzymes. The reaction catalyzed by ACC2 is itself activated by citrate (see Figure 1) [60]. By activating ACC2, citrate also indirectly inhibits the β-oxidation, and thereby positively regulates the FADNS pathway [73,74]. Besides, the ACC enzymes are allosterically repressed by malonyl-CoA, long-chain fatty acyl-CoA, and free CoA [66,75,76]. Both ACC isoforms are also subject to diet and hormonal regulations [60,77–79]. In addition, magnesium, in the form of Mg^{2+}, facilitates the transfer of the carboxyl group of the ATP to the biotin coenzyme, and stabilizes the transition state during the first step of the malonyl-CoA synthesis reaction (carboxylation reaction) [80]. Thus, Mg^{2+} is a cofactor for the reaction and it influences its kinetics.

Our current understanding of the ACC mechanism is based on several studies that have been reviewed by Numa and Tanabe [74]. Using isotope labeling, the three steps of the mechanism could be characterized. Also, Hashimoto et al. [81] suggested an ordered Bi Bi Uni Uni Ping Pong mechanism with an activation by citrate. The order of attachment of the substrates to the enzyme is, ATP, HCO_3^-, and acetyl-CoA for the forward reaction, and malonyl-CoA, Pi, and ADP for the reverse reaction [81]. The reaction is subject to product regulation, notably by malonyl-CoA and ADP. The mathematical expression of the rate law, including numerical values of the kinetic parameters, has been reported by Hashimoto et al. [81]. With 16 parameters, it is quite complex, although it does not include inhibition by long-chain acyl-CoAs. The reaction mechanism was later questioned by Beaty and Lane [82], and Kaushik et al.

Table 2 Kinetic parameters of ACC isoenzymes

ACC												
Organism /Source	Substrate	Activator	Inhibitor	K_m	k_{cat}	K_a	K_i	pH	Temperature	Measurement approach	Remarks	Reference
Rat hindlimb muscle	Acetyl-CoA	Citrate	Malonyl-CoA	31.7 ± 1.5 μM		2.13 ± 0.05 mM	10.6 ± 1 μM	7.5	37°C	^{14}C-labeled $KHCO_3$ radioactivity-based assay; thekinetic parameters were measured by using the Line weaver-Burk plot method	Purified enzyme Unknown isoform	[68]
	ATP		C16:0-CoA	57.6 ± 0.9 μM			2.2 ± 0.3 μM					
	$KHCO_3$			2.25 ± 0.1 mM								
Rat adipose tissue	Acetyl-CoA	Citrate		21.5 ± 1 μM		3.02 ± 0.12 mM						
	ATP			106.5 ± 2.6 μM								
	$KHCO_3$			2.73 ± 0.29 mM								
Human ACC1	Acetyl-CoA			34 ± 4 μM	10.1 ± 1.2 s^{-1}			7.5	37°C	^{14}C-labeled $NaHCO_3$ radioactivity-based assay; the kinetic parameters were measured by non-line arregression fitting to Michaelis-Menten equations	Purified recombinant enzyme expressed in baculovirus; the ACC2 lacks the N-terminal 148 aa region; the malonyl-CoA exerts a competitive in hibition	[66]
	ATP			161 ± 31 μM								
	NaHCO3			12.8 ± 0.7 mM								
Human ACC2	Acetyl-CoA			58 ± 17 μM	11.8 ± 3.8 s^{-1}							
	ATP			120 ± 15 μM								
	$NaHCO_3$			3.0 ± 0.8 mM								
Rat ACC2	Acetyl-CoA			37 ± 12 μM	11.6 ± 2.4 s^{-1}							
	ATP			147 ± 13 μM								
	$NaHCO_3$			5.1 ± 0.3 mM								
Human ACC2 (27-2458)	Acetyl-CoA			2 ± 0.2 μM	11.5 ± 2.0 min^{-1}			7.5	25°C	^{14}C-labeled acetyl-Co Aradioactivity-based assay; the kinetic parameters were measured by fitting data to Michaelis-Menten equation	The enzyme is expressed in baculovirus; the ACC2 are truncated (lacking 1–148aa), or N-terminal 275 aa is replaced with the ACC1 region (1-33aa)	[134]
	ATP			52.3 ± 4.4 μM	9.3 ± 2.0 min^{-1}							
Human ACC2 (21-2458)	Acetyl-CoA			2.6 ± 0.8 μM	17.8 ± 1.6 min^{-1}							
	ATP			43.7 ± 3.5 μM	13.7 ± 0.5 min^{-1}							

Cells are empty when the parameter values were either not measured or not considered in the rate laws. The meaning of each symbol is defined in the List of Symbols.

Bioscience Reports (2023) **43** BSR20222496
https://doi.org/10.1042/BSR20222496

Table 3 Kinetic parameters of FAS

FAS & active sites

Organism/Source	Substrate	Activator	Inhibitor	K_m	kcat	K_a	Ki	pH	Temperature	Measurement approach	Remarks	Reference
Chicken Liver (full enzyme)	Acetyl-CoA	CoA	Malonyl-coA	0.2 μM	10.4 ± 0.7 s^{-1}		1.2 μM	5.90	25°C	Spectrophotometry-based assay by following the reduction of NADPH absorbance	Purified enzyme; although it was shown that the free CoA at low concentration activates the enzyme and at high concentration inhibits the enzyme, the value of the corresponding constants are not reported, the reported parameters correspond to the formation of 16:0	[34]
	Malonyl-CoA		Acetyl-CoA	1.7 ± 0.3 μM			6.0 ± 1.3 μM					
	NADPH			2.0 ± 0.8 μM								
	Acetyl-CoA		Malonyl-CoA	0.25 μM	10.4 ± 0.7 s^{-1}		1.9 μM	6.56				
	Malonyl-CoA		Acetyl-CoA	1.6 ± 0.4 μM			5.0 ± 1.3 μM					
	NADPH											
	Acetyl-CoA		Malonyl-CoA	0.72 ± 0.17 μM	23.0 ± 0.7 s^{-1}		3.1 ± 0.8 μM	7.0				
	Malonyl-CoA		Acetyl-CoA	2.5 ± 0.8 μM			5.4 ± 0.6 μM					
	NADPH			2.9 ± 0.4 μM								
	Acetyl-CoA		Malonyl-CoA	0.85 ± 0.27 μM	17.0 ± 0.9 s^{-1}		4.0 ± 0.4 μM	7.49				
	Malonyl-CoA		Acetyl-CoA	4.3 ± 0.6 μM			10.4 ± 1.5 μM					
	NADPH											
	Acetyl-CoA		Malonyl-CoA	1.9 ± 0.5 μM	11.0 ± 1.0 s^{-1}		16.3 ± 11 μM	8.0				
	Malonyl-CoA		Acetyl-CoA	5.7 ± 1.0 μM			16.9 ± 3.2 μM					
	NADPH			3.5 ± 0.8 μM								
	Acetyl-CoA		Malonyl-CoA	2.9 ± 0.4 μM	4.0 ± 0.2 s^{-1}		60.0 ± 30 μM	8.60				
	Malonyl-CoA		Acetyl-CoA	5.5 ± 0.9 μM			19.0 ± 4.5 μM					
	NADPH			5.0 ± 0.6 μM								

Continued over

Table 3 Kinetic parameters of FAS (Continued)

FAS & active sites

Organism/Source	Substrate	Activator	Inhibitor	K_m	k_{cat}	K_a	K_i	pH	Temperature	Measurement approach	Remarks	Reference
Human (full enzyme)	Acetyl-CoA			7 ± 3 μM	2.7 ± 0.25 s^{-1}			7.0	25°C	Spectrophotometry-based assay by following the reduction of NADPH absorbance	Purified enzyme expressed in baculovirus	[92]
	Malonyl-CoA			6 ± 2 μM								
	NADPH			5 ± 1 μM								
β-ketoacyl reductase site (human)	Acetoacetyl-CoA			10 ± 2 μM	4 ± 0.2 s^{-1}							
	NADPH			4 ± 2 μM								
β-hydroxyacyl dehydratase site (human)	Crotonyl-CoA (4:0)			7 ± 5 μM	0.1 ± 0.02 s^{-1}							
Enoyl-reductase site (human)	Crotonyl-CoA (4:0)			6 ± 2 μM	0.3 ± 0.03 s^{-1}							
	NADPH			3 ± 2 μM								
Enoyl-reductase site (human)	Octenoyl-CoA (8:0)				0.05 ± 0.02 s^{-1}							
	NADPH			100 ± 70 μM								
Enoyl-reductase site (human)	Dodecenoyl-CoA (12:0)			7 ± 1 μM	0.22 ± 0.08 s^{-1}							
	NADPH			540 ± 300 μM								
Malonyl-acetyl-transferase site (human)	Acetyl-CoA			3.9 ± 0.4 μM	1.9 ± 0.06 s^{-1}			6.8	0°C	Radioactivity-based assay combined with liquid chromatography using either ^{14}C-labeled acetyl-CoA or malonyl-CoA	Purified enzyme expressed in *Escherichia coli*	[89]
Malonyl-acetyl-transferase site (rat liver)	Malonyl-CoA			1.9 ± 0.23 μM	1.2 ± 0.008 s^{-1}							

Cells are empty when the parameter values were either not measured or not considered in the rate laws. The meaning of each symbol is defined in the List of Symbols.

Bioscience Reports (2023) **43** BSR20222496
https://doi.org/10.1042/BSR20222496

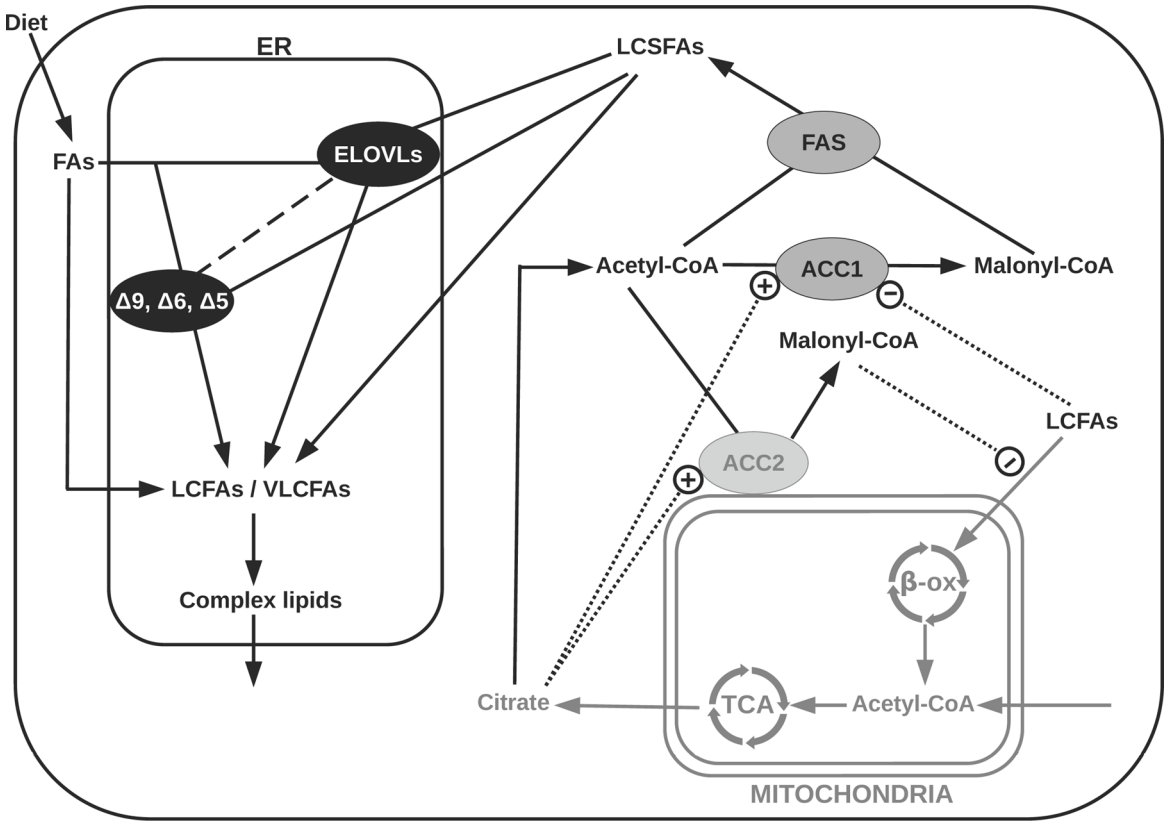

Figure 1. Schematic representation of the biochemistry of fatty acid biosynthesis

The process is organized in two main parts. Enzymes involved in the FADNS (FAS and ACC1) are color-coded with a gray background. They are responsible for the production of long chain saturated fatty acids (LCSFAs). This process takes place in the cytoplasm. Enzymes involved in the microsomal modifications of fatty acids (ELOVLs, Δ-desaturases) are color-coded with a black background. They are responsible for elongating and desaturating long-chain fatty acids (LCFAs) and very long-chain fatty acids (VLCFAs). This process takes place in the endoplasmic reticulum (ER) where these enzymes are membrane-bound. In the ER, LCFAs and VLCFAs, represented on the figure, include LCSFAs, monounsaturated FAs (MUFAs), and polyunsaturated FAs (PUFAs). The β-oxidation that takes place in the mitochondria is not part of the fatty acid synthesis. Still, it is represented because it influences the overall synthesis process. For the sake of simplicity, several enzymes and transporters that are not directly involved in the synthesis are not represented, e.g., malonyl-coA decarboxylase, fatty acid-binding proteins, and acyl-CoA-binding proteins.

[67], who instead proposed the random Ter Ter mechanism. Both articles provide detailed kinetic parameter values, useful for the construction of models. Liquid chromatography/mass spectrometry/mass spectrometry (LC/MS/MS) data of malonyl-CoA formation were fitted to the proposed rate law, allowing characterizing the human recombinant ACC2 [67]. The resulting kinetic parameters resemble those reported for rat skeletal muscle [68] and human recombinant enzymes [66]. Besides, Ogiwara et al. [75] and Tanabe et al. [83] focused on the inhibition constants of natural inhibitors (both substrate and product inhibitions) in rat liver. For example, Tanabe et al. [83] reported the inhibition constants of LCFAs and analogs. Inhibition constants for malonyl-CoA and palmitoyl-CoA were also determined [68].

FAS

FAS is the cytosolic homodimeric multifunctional enzyme responsible for the channeled elongation reactions in the FADNS [84–86] (see Figure 1). This enzyme comprises seven catalytic sites, including the ACP domain that is responsible for channeling. The reaction is initiated from acetyl-CoA with malonyl-CoA as carbon donor for elongation, and NADPH as reducing equivalent. The elongation cycle takes place in four steps: condensation, reduction, dehydration, and reduction [2]. The thioesterase site releases the final products of the FADNS, mainly 16:0. This suggests

a high selectivity of the thioesterase domain for the 16:0-intermediate, which was confirmed by Chakravarty et al. [87] in *in vitro* experiments.

Two main strategies are reported in the literature for the derivation of the FAS kinetic rate law: (i) considering each elementary reaction till the production of a LCSFA [34,88–90]; or (ii) lumping all the steps up to the production of a LCSFA as a single reaction [91,92]. The common feature of the studies using either approach is that acetyl-CoA and malonyl-CoA compete for the same enzyme-binding site.

Studying the mechanism of elongation by focusing on each of the seven enzymatic sites, Katiyar et al. [88] concluded that all the individual reactions follow a Ping Pong mechanism except the reduction steps [88]. The latter were suggested to instead follow random sequential or ordered sequential mechanisms, with NADPH added first, and the proton added second [88]. From these individual steps, the overall kinetic rate law of FADNS was derived using the King and Altman's method [38]. The resulting detailed rate law has 11 parameters. This complexity may make it difficult to fit the kinetic parameters and to relate them to their biological meaning. In chicken liver, Cox and Hammes [34] proposed a simpler rate law for the overall reaction, following a three substrates Michaelis–Menten kinetics, with competition of acetyl-CoA and malonyl-CoA. They described the associated mechanism with eight elementary steps. The first two correspond to the attachment of acetyl-CoA to the enzyme. Steps 3 to 7 repeat at each elongation cycle, while step 8 is the release of the final product, chosen as palmitic acid (16:0). In their approach, all complex formation involving CoA or NADPH are reversible, characterized by their dissociation constant. Moreover, the authors highlighted the explicit relation between the mechanistic parameters (kinetic rate constants and dissociation constants), and the k_{cat} and K_{m_i} (i is either acetyl-CoA, malonyl-CoA, or NADPH) of the overall kinetics. k_{cat} and K_{m_i} were measured at various pH-values, thereby highlighting the impact of this experimental condition on the efficiency of the enzyme (k_{cat}/K_{m_i}).

Other studies employ a twofold approach, to first lump the reactions and derive the rate law, and second measure detailed kinetic parameters for specific reaction steps. For instance, Carlisle-Moore et al. [92] considered a lumped reaction for the production of 16:0 in human, and measured the k_{cat} and K_{m_i}-values (i is either acetyl-CoA, malonyl-CoA, or NADPH). Then, the same parameters were determined for the reduction and dehydration steps, when considered separately. In particular, those of the enoyl-CoA reductase site (last one of the elongation cycle) were assessed as a function of the substrate chain length (4:0, 8:0, and 12:0) (see Table 3). A similar approach was followed in chicken liver using tracer experiments in order to determine V_{max} and K_{m}-values for various substrates [91].

In vitro measurements of the FAS kinetics suffer from limitations, e.g., the malonyl-CoA decarboxylation into acetyl-CoA, and the natural abundance of the ^{13}C carbons that introduces extra noise in the case of ^{13}C MS assays. Their impact was observed in kinetic assays by Ohashi et al. [93] and Topolska et al. [57], using enzymes from guinea pig harderian gland and cow, respectively.

Microsomal modifications of FAs

Metabolic functions require specific FA profiles [94,95]. Some FAs cannot be synthesized *de novo* (essential FAs) and, therefore, must be obtained from external sources. The FAs produced *de novo* (endogenous) and those from the diet (exogenous) are not always suitable, and must be modified accordingly. This modification takes place in the ER and involves two processes, elongation and desaturation. Those are synergized to ensure FA diversity and specific profiles. Elongation produces VLCFAs. They are essential precursors for various classes of lipids, such as phospholipids, sphingolipids, triglycerides, cholesterol esters, and wax esters, whose synthesis are beyond the scope of the present review [96]. Desaturation tunes FA properties [97]. For instance, the cellular and organellar membrane permeability and fluidity depend on the level of unsaturation of their constitutive FAs [98]. Below, we introduce the biochemistry of each enzyme. For the sake of briefness, we also provide tables that summarize the main biochemical characteristics of elongases (see Table 4) and desaturases (see Table 5). For further details, the reader is referred to [99–101] for elongases and [97,99,102] for desaturases. In addition, like in section 2, we tabulated some of the associated kinetic parameters for the reader to construct the respective kinetic rate laws (see Tables 6–8).

Elongases

The microsomal elongation of FAs is the major pathway to produce VLCFAs [103]. Similarly to the *de novo* synthesis, it utilizes malonyl-CoA and NADPH as carbon donor and reducing agent, respectively. The microsomal elongation process consists of four steps: condensation, reduction, dehydration, and reduction. The end product of the elongation is an acyl-CoA with two extra carbons. Unlike the *de novo* synthesis, each step is catalyzed by a distinct enzyme. To date, seven 3-keto-acyl-CoA synthases catalyzing the condensation step have been identified in mammals, the so-called elongation of very long-chain fatty acids (ELOVLs) enzymes [104]. They are membrane bound and located at the surface of the ER (see Figure 1). Besides, unlike the other three enzymes involved in the microsomal elongation

Bioscience Reports (2023) **43** BSR20222496
https://doi.org/10.1042/BSR20222496

Table 4 Summary on biochemistry of elongases

Enzyme	Tissue expression	Substrate type	Substrate chain length	References
ELOVL 1	almost all tissues	SFAs and MUFAs	18–26	[96,135–137]
ELOVL 2	testis^{+}, liver^{+}, brain^{-}, kidney^{-}, WAT^{-}, lung^{-}	essential PUFAs, preference for nonessential FAs in mouse	20–22	[96,136–139]
ELOVL 3	skin sebaceous gland, hair follicles, BAT	SFAs, USFAs	16–22	[96,109,136,137]
ELOVL 4	retina, brain, skin, testis^{+}, prostate^{+}, ovary, thymus^{+}, small intestine^{+}	SFAs, ULCFAs	$\geq$ 24	[96,136]
ELOVL 5	almost all tissues	essential PUFAs	18–20	[96]
ELOVL 6	almost all tissues	12:0, 14:0, 16:0, 16:1n7, 18:1n9	12–18	[96,138,140,141]
ELOVL 7	brain^{-}, liver^{-}, small intestine^{-}, testis^{-}, leukocytes^{-}, placenta^{-}, colon^{+}, kidney^{+}, prostate^{+}, pancreas^{+}, adrenal glands^{+}	16:0, 18:0, 20:0, 18:1n9, 18:3n6 preference for nonessential FAs	16–20	[96,109,142]

The symbols "+" and "−" on top of tissues, respectively, mean highly expressed and poorly expressed in the corresponding tissue. If no sign is indicated, the information could not be retrieved from the literature. All acronyms used here are listed in the Abbreviation subsection.

Table 5 Summary on biochemistry of desaturases

Enzyme	Isoforms	Substrates	Tissue specificity	Regulators	Biological function	References
Δ9	SCD1 ^{m,h}	14:0, 16:0, 18:0*	lipogenic tissues (e.g., liver and adipose tissues)	HCD $^{+}$, SFAs $^{+}$, insulin $^{+}$, estrogen $^{+}$, liver X receptors $^{+}$, PPAR α $^{+}$, glucagon $^{-}$, PUFAs $^{-}$, leptin $^{-}$	desaturate LCSFAs	[114,118,143–148]
	SCD2 ^{m}		brain, pancreas			[114,118,143,148]
	SCD3 ^{m}	16:0 only (SCD3)	harderian, sebocytes, preputial glands			[114,118,143,149]
	SCD4 ^{m}		heart			[114,118,143,147]
	SCD5 ^{h}		brain, pancreas			[114,118,143,148]
Δ6	FASD1	16:0$^{\#}$, 18:2n-6, 18:3n-3, 24:5n-3	skin $^{+}$, liver $^{+}$, brain $^{+}$, heart $^{\pm}$, lungs $^{\pm}$, kidney $^{-}$, spleen $^{-}$, muscles $^{-}$	PUFAs $^{+}$	build HUFAs, build 16:1n7 found in human sebum	[97,115,116,125]
Δ5	FASD2	20:3n-6, 20:4n-3	liver $^{+}$, brain $^{+}$, heart $^{\pm}$, lungs $^{\pm}$, kidney $^{-}$, spleen $^{-}$, muscles $^{-}$	PUFAs $^{+}$	build HUFAs	[97,115,116,125]

In the isoforms column, *m* and *h* mean present in mice and humans, respectively. In the substrates column, '*' indicates the preferred substrate, while '#' indicates a special case of desaturation. In the tissue specificity column, '+' and '−' indicate that the enzyme is highly or lowly expressed, respectively, while '±' means moderately expressed in the corresponding tissue. In the regulators column, '+' and '−' indicate enzyme activity increase and decrease, respectively. All acronyms used here are listed in the Abbreviation subsection.

process (i.e., 2,3-*trans*-enoyl-CoA reductase, 3-keto-acyl-CoA reductase, and 3-hydro-acyl-CoA dehydratase), the ELOVLs are substrate specific, catalyze the rate-limiting step, and are differently expressed in distinct tissues (see Table 4). Hence, they play a central role in determining the distribution of VLCFAs [96,99,100,104–106], and so we choose to focus on them.

Bioscience Reports (2023) **43** BSR20222496
https://doi.org/10.1042/BSR20222496

Table 6 Kinetic parameters of elongases

Elongation cycle/ELOVLs												
Organism/Source	**Substrate**	**Activator**	**Inhibitor**	K_m	V_{max}	K_a	K_i	**pH**	**Temperature**	**Measurement approach**	**Remarks**	**Reference**
Porcine purified microsomes	Malonyl-CoA			32.5 μM	1.6 nmol · h^{-1} · mg^{-1}			7.5		Radioactivity-based assay combined with ^{14}C labeled malonyl-CoA	Purified microsomes containing all the enzymes responsible for the elongation cycle	[108]
	16:0-CoA											
	NADPH			9.1 μM	1.2 nmol · h^{-1} · mg^{-1}							
Porcine purified microsomes	Malonyl-CoA			12.9 μM	0.8 nmol · h^{-1} · mg^{-1}							
	20:0-CoA											
	NADPH			23.8 μM	0.67 nmol · h^{-1} · mg^{-1}							
ELOVL7 (human)	Malonyl-CoA			11.7 μM	0.31 pmol · min^{-1} · μg^{-1}			6.8	37°C	Radioactivity-based assay combined with ^{14}C labeled malonyl-CoA	Reconstituted purified enzyme using the proteoliposome-reconstitution system	[109]
	18:3n-3-CoA			2.6 μM	0.33 pmol · min^{-1} · μg^{-1}							
ELOVL6 (human)	Malonyl-CoA			6.46 μM	1.03 pmol · min^{-1} · μg^{-1}			6.8	37°C	Radioactivity-based assay combined with ^{14}C labeled malonyl-CoA	Reconstituted purified enzyme using the proteoliposome-reconstitution system	[110]
	16:0-CoA			1.22 μM	0.79 pmol · min^{-1} · μg^{-1}							

It is important to recall that the purified microsomes are not the purified enzymes. They contain the four enzymes of the elongation cycle, together with other enzymes that could impact their kinetics. The concentration of each elongation enzyme therefore remains unknown. Cells are empty when the parameter values were either not measured or not considered in the rate laws. The meaning of each symbol is defined in the List of Symbols.

Bioscience Reports (2023) **43** BSR20222496
https://doi.org/10.1042/BSR20222496

Table 7 Kinetic parameters of Δ9 desaturase

Δ9 desaturase

Organism/Source	Substrate	Activator	inhibitor	K_m	k_{cat}	K_a	K_i	pH	Temperature	Measurement approach	Remarks	Reference
Rat liver microsome	C18:0-CoA			10.5 μM				7.4	37°C	^{2}H-labeled C18:0-CoA mass spectrometry approach (RF-MS), Lineweaver-Burk plot	Not the purified enzyme	[122]
	NADH											
Bovine mammary microsome	C18:0-CoA			25 μM				7.4	30°C	^{14}C labeled C18:0-CoA radioactivity-based method, Lineweaver-Burk plot	Not the purified enzyme	[123]
	NADH			3 μM								
Rat liver	14-19 carbon chain acyl-CoAs			4.5 – 5 μM					25°C	Radioactivity-based assay using ^{14}C- labeled substrates	Purifiedenzyme; the exact names of the acyl-CoAs are not specified	[124]

Cells are empty when the parameter values were either not measured or not considered in the rate laws. The meaning of each symbol is defined in the List of Symbols.

Table 8 Kinetic parameters of Δ5 and Δ6 desaturases

Δ5 and Δ6 desaturases

Organism/Source	Substrate	Activator	Inhibitor	K_m	V_{max}	K_a	K_i	pH	Temperature	Measurement approach	Remarks	Reference
Δ6 human fetal liver	18:2n-6-CoA			6.5 μM	7.5 pmol · min^{-1} · mg^{-1}			7.4	37°C	Radioactivity-based assay using ^{14}C-labeled substrates; Lineweaver-Burk plot	Not a purified enzyme; liver microsomes from human fetus	[127]
	18:3n-3-CoA			24.5 μM	24.4 pmol · min^{-1} · mg^{-1}							
Δ5 human fetal liver	20:3n-6-CoA			3.91 μM	9.5 pmol · min^{-1} · mg^{-1}			7.4	37°C	Radioactivity-based assay using ^{14}C-labeled substrates; Lineweaver-Burk plot	Not a purified enzyme; liver microsomes from human fetus	[127]
Δ5 rat kidney	20:3n-6-CoA			56 μM	60 pmol · min^{-1} · mg^{-1}			7.0	36°C	Radioactivity-based assay using ^{14}C-labeled substrates; Lineweaver-Burk plot	Not a purified enzyme; rat kidney microsomes	[128]
Δ6 rat liver	18:2n-6-CoA			45 μM	83 nmol · min^{-1} · mg^{-1}			7.2	30°C	Radioactivity-based assay using ^{14}C-labeled substrates; Lineweaver-Burk plot	Purified enzyme	[126]

Cells are empty when the parameter values were either not measured or not considered in the rate laws. The meaning of each symbol is defined in the List of Symbols.

The analysis of the kinetics of the microsomal elongation began with the pioneering work by Nugteren [107] using rat liver microsomes. They ^{14}C-labeled malonyl-CoA, long-chain saturated and unsaturated FAs, and intermediates. They studied the overall elongation cycle by deriving the normalized rate of elongation, as a function of the chain length and degree of unsaturation of the substrates. They also reported detailed time-course data for the overall elongation of 14:0 to 16:0. A similar approach was carried out three decades later, using porcine neutrophil microsomes, assuming that the elongation follows a Michaelis–Menten rate law. It was possible to determine V_{max} and K_m-values for malonyl-CoA and NADPH for 16:0-CoA and 20:0-CoA, as well as the overall activity for the elongation cycle [108]. Although at that time, ELOVLs were not yet clearly identified, these studies paved the way for investigating their kinetics. Surprisingly, the latter has been little investigated since ELOVLs were identified in the early 2000s. The most popular studies are by Naganuma et al. [109], and Naganuma and Kihara [110] on ELOVL7 and ELOVL6, respectively. In both, the kinetic parameters of the enzyme were determined using HEK 293T cells. For ELOVL7, these were V_{max} and K_m-values for malonyl-CoA and 18:3n-3-CoA. For ELOVL6, the corresponding values were determined for malonyl-CoA and 16:0-CoA. Neither ELOVL7 nor ELOVL6 are subject to allosteric inhibition; however, ELOVL6 is repressed by PUFAs [111]. Besides, Naganuma and Kihara [110] showed that NADPH and 3-ketoacyl-CoA reductase enhance the activity of ELOVL7. The underlying mechanism is unknown, but they speculated that the presence of the 3-ketoacyl-CoA reductase may cause a conformational change of the enzyme, thereby increasing its activity. This hypothesis could for instance be tested using fluorescent nanoantennas that allow monitoring small and large protein conformational changes [112].

Desaturases

The desaturase enzymes are responsible for the introduction of double bonds at specific positions along FA chains. Like the ELOVLs, they are membrane-bound enzymes and are located in the ER (see Figure 1). They are substrate and tissue-specific [99]. Desaturation tailors FA properties (e.g., melting point, rancidity, and flexibility) that ensure their suitability for various biological processes [97]. In mammals, three desaturases have been identified, namely the Δ5 desaturase, the Δ6 desaturase, and the Δ9 desaturase [97,113]. The three desaturations follow the same mechanism. The ΔX desaturation consists in introducing a *cis* double bond between the carbons X and $X + 1$, counted from the carboxyl end. Via a series of reactions, the ΔX desaturase consecutively removes two hydrogen atoms, the first one at the X^{th} position, and the second one at the $X + 1^{\text{th}}$ position [113–116]. These two hydrogens are combined with molecular oxygen and released as water [117]. The electrons required for this reduction are derived from cytochrome b_5 [114–116]. One should note that for unsaturated FAs, a further desaturation does not change the nY family to which the FA belongs, Y being the position of the first double bond, counted from the methyl-end. Further biochemistry details of the ΔX enzymes are summarized in Table 5, i.e., their isoforms, substrates, tissue specificity, regulators, and biological functions. As for their kinetic features, very little information and data are available. This may be due to particularly challenging experimental tractability. Specifically, here we are dealing with membrane-bound enzymes, whose purification requires several complicated steps. Furthermore, the desaturation reactions involve an intermediate step catalyzed by an extra enzyme (i.e., cytochrome b_5 reductase), making the design of kinetics assays difficult.

Δ9 Desaturase

The MUFAs play a crucial role in lipid homeostasis and the physiological functions of lipids [117–119]. To ensure their presence in an adequate proportion, they are endogenously produced from saturated FAs by the Δ9 desaturase, also known as stearoyl-CoA desaturase (SCD). Ntambi et al. [120] and Miyazaki et al. [121] reported that SCD-deficient mice show an increase in insulin sensitivity and are protected against diet-induced adipocity. This suggests that the Δ9 desaturase could be a good therapeutic candidate for obesity and metabolic syndromes. Yet, the literature turns out to be less furnished with respect to the kinetic features of the Δ9 desaturase, as compared with those of the FADNS enzymes. Specifically, the kinetics associated to the detailed mechanism of the enzyme is not discussed. Thus, as a first intention, most studies assume a Michaelis–Menten rate law. Three studies following this approach in mammals can be stressed. They respectively use rat liver microsomes [122], bovine mammary microsomes [123], and purified rat liver enzyme [124], and provide a starting point for kinetic modeling. Since the first two studies do not use purified enzymes, the k_{cat} values cannot be determined. As an alternative, one can use the Lineweaver-Burk plot of the kinetic data, together with the mass of the protein, to infer the V_{max} values. For example, from the data of Soulard et al. [122], we can estimate the V_{max} values to be about 2 $\mu\text{M} \cdot \text{min}^{-1} \cdot \text{mg}^{-1}$ protein and 1.17 $\mu\text{M} \cdot \text{min}^{-1} \cdot \text{mg}^{-1}$ protein, for 18:0 and NADH, respectively. When considering the study by Strittmatter and Enoch [124], it appears that its purpose is not to measure the kinetic parameters, but to present in detail the procedure of purification of the enzyme. Hence, in that case, we can infer neither the k_{cat} nor the V_{max} values from the reported data. Despite the limited information available in the literature, the reader can take into account the K_{m} values tabulated in order to begin developing a kinetic model (see Table 7). We believe that a subsequent effort should be placed into measuring the kinetic parameters of the Δ9 desaturase, notably the k_{cat} and K_{m} values for the different substrates, and the parameters associated with potential regulatory mechanisms.

Δ5 and Δ6 desaturases

The n3 and n6 FA families (also known as ω3 and ω6) are unsaturated essential FA precursors for the synthesis of highly unsaturated FAs (HUFAs). The latter are involved in cell membrane composition, signaling processes, brain and retina development, and cognition and inflammatory responses [97,113]. Animals cannot synthesize *de novo* ω3 and ω6 FAs, but can modify the essential FAs 18:3n3 and 18:2n6 acquired from external sources to fit the adequate fatty acid profiles. The Δ5 and Δ6 desaturases are required for this modification [97,115,116]. Like the ELOVLs and Δ9 desaturase, the Δ5 and Δ6 desaturases are membrane-bound enzymes. Interestingly, the Δ6 desaturase, highly expressed in the skin, has been shown to act on the saturated FA 16:0, resulting in the MUFA 16:1n-10. This special case is highlighted by the symbol # in Table 5. This finding is consistent with the fact that 16:1n-10 is the major FA, found in human sebum [125].

Like for the Δ9 desaturase, the kinetics of animal Δ5 and Δ6 desaturases is understudied. Furthermore, only a few studies use purified enzymes. For instance, Okayasu et al. [126] used the purified Δ6 desaturase from rat liver to measure K_{m} and V_{max} values for 18:2n-6-CoA. Opposite, Rodriguez et al. [127] focused on the kinetics of both Δ5 and Δ6 desaturases using human fetal microsomes. The K_{m} and V_{max} values were measured for 20:3n-6-CoA for Δ5,

Bioscience Reports (2023) **43** BSR20222496
https://doi.org/10.1042/BSR20222496

and 18:2n-6-CoA and 18:3n-3-CoA for Δ6. In addition, Irazú et al. [128] measured the K_m and V_{max} values of Δ5 using rat kidney microsomes. For these three studies, a summary of the parameter values, as well as the conditions of measurement, are provided in Table 8. In the table, the kinetic parameters are only reported for essential FAs. One should also note that, although in all these *in vitro* studies the authors report substrate inhibition when the substrates are above a certain threshold, we choose to not tabulate them, since this phenomenon is unlikely to be observed *in vivo*. Finally, nothing is known about the kinetics of desaturation of 16:0 by the Δ6 desaturase.

Discussion and conclusions

FAs are the precursors of lipid synthesis, and therefore fundamental building blocks in every living cell. It is thus not surprising that many metabolic disorders are associated with defects in FA metabolism [60,129]. Mathematical modeling has become an increasingly popular approach for the investigation of biochemical pathways. Model simulations can guide experiments and support the identification of potential drug targets. Their construction relies on the availability of experimental data concerning the detailed enzymatic mechanisms, the enzyme kinetics, the associated mathematical rate laws, and the values of the corresponding parameters. In the present review, we focused on animal fatty acid synthesis with a particular emphasis on mammals. We aimed to summarize the information necessary for constructing dynamic mathematical models describing this complex enzymatic process using rate laws. We first gave an overview of the framework, and then reviewed the kinetic information of the enzymes involved, including both the FADNS and the microsomal modification pathways. We also provided tables summarizing the kinetic information, as well as the basic biochemistry, of the enzymes involved (Tables 2–8). Throughout, we report facts and figures for each enzyme individually. To calibrate a model encompassing the entire fatty acid synthesis pathway, the reader may also be interested in the *in vivo* data collected by Hems et al. [130] in the liver and the adipose tissues of lean and obese mice.

We find that, despite enormous amount of available information and data, our knowledge is still limited. Most of the enzymes involved in animal fatty acid synthesis are membrane bound, which makes it extremely challenging to systematically analyze their kinetics in controlled *in vitro* experiments. For instance, the purification of such enzymes requires their solubilization, which may lead to an alteration or even a complete loss of their activity [109]. Furthermore, this step is particularly tedious, which possibly explains why most studies that we reviewed instead use recombinant proteins or cell extracts. Remarkably, recent approaches have shown successes in characterizing membrane-bound enzymes by embedding them into liposomes, mimicking their natural environment [109,131]. Even if these techniques are further developed to allow for systematic determination of kinetic parameters, it still has to be considered that an *in vitro* system never precisely reflects the situation *in vivo*. The conditions of *in vitro* assays, both physical (e.g., pH, temperature) and chemical (e.g., buffer) can influence the measured kinetic parameter values, due to suboptimal enzymatic conformation changes during the reaction. Besides, the complexity of the enzymatic process itself can limit the development of new assays. That is for instance the case of the ΔX desaturation process that includes a reduction step involving an extra enzyme, cytochrome b_5 reductase. Furthermore, the unavailability of the purified native enzyme may lead to *in vitro* experiments based on either truncated or recombinant enzymes, or cell extracts. Still, it is unclear whether any of these substitutes can be considered as a good proxy for their native counter-part. When kinetic data are unavailable, in order to develop a mathematical model, an alternative is to use information from a distinct tissue or isoform, or an orthologous protein from a closely related organism. We showed in particular the similarities observed by Cheng et al. [66] for the values of the kinetic parameters for the ACC enzymes. Still, one cannot generalize such alikeness, and it is important to carefully consider the limits of these approximations. Although Cox and Hammes [34] provided detailed kinetic information on FAS from chicken liver, we can similarly question whether the derived parameter values reflect those in mammals. Naturally, ethical concerns restrict the possibility to perform *in vivo* experiments in humans. Therefore, alternative methods focusing on simpler systems appear as promising technologies to better mimic *in vivo* conditions. They, for instance, consist in cultivating specific cell lines (e.g., adipocytes and hepatocytes) or grow organ on chips [132,133].

It is currently feasible to build mathematical and computational models of animal fatty acid synthesis based on available kinetic information. However, literature gaps present a major obstacle for developing a more fundamental understanding of these pathways, which may considerably impair research progress, and its implications in the medical domain. To overcome these limitations, it will not be sufficient to simply perform more experiments, but it will also be necessary to find unifying standards to test, report, and store this important wealth of data in a findable and reusable manner. Additionally, we must take advantage of the growing field of targeted metabolomics, utilizing techniques such as stable isotope labeling, for measuring the kinetic parameters both *in vitro* and *in vivo*.

Perspectives

- **Highlight importance of the field:** Fatty acid metabolism is essential for mammals and is associated with several disorders, some of which are severe societal burdens. To tackle these challenges, mathematical and computational models are increasingly important. They allow to test specific hypothesis, make predictions, rationalize experimental and medical data, and guide the design of new experiments.
- **Summary of the current thinking:** Enzymes involved in the fatty acid *de novo* synthesis have received far more attention than those in the microsomal modification. In addition, several limitations must be taken into consideration when developing a mathematical model. Most experiments are performed *in vitro*, purified native enzymes are rarely investigated, and data are so scarce that it is impossible to gather a complete set of kinetic data for a single organism.
- **Comment on future directions:** To overcome these limitations, we suggest studying enzyme kinetics using a dual approach combining both experiments and mathematical models. Furthermore, we stress the need for a systematic and standardized reporting of kinetic information, and suggest to further take advantage of the growing field of targeted metabolomics to measure kinetics both *in vitro* and *in vivo*.

Competing Interests

The authors declare that there are no competing interests associated with the manuscript.

Funding

This paper was supported by the European Union's Horizon 2020 research and innovation program under the Marie Sklodowska-Curie grant agreement PoLiMeR [number 812616]. To complete this work, the position of A.R. was funded by the Federal Ministry of Education and Research of Germany in the framework of CornWall [Project Number 031B0193A], and the German federal and state program Professorinnenprogramm III for female scientists. This work was funded by the Deutsche Forschungsgemeinschaft (DFG, German Research Foundation) under Germany's Excellence Strategy [EXC-2048/1 project ID 390686111].

CRediT Author Contribution

Chilperic Armel Foko Kuate: Conceptualization, Investigation, Visualization, Methodology, Writing—original draft, Writing—review & editing. **Oliver Ebenhöh:** Supervision, Funding acquisition, Writing—review & editing. **Barbara M. Bakker:** Supervision, Funding acquisition, Writing—review & editing. **Adélaïde Raguin:** Conceptualization, Supervision, Funding acquisition, Visualization, Methodology, Writing—original draft, Writing—review & editing.

Acknowledgements

The authors acknowledge the support of Jasmin Theilmann in formatting the paper.

Appendix A Symbols

List of Symbols	
A	Activator
I	Inhibitor
K_m	Michaelis–Menten constant
K_a	Activation constant
K_i	Inhibition constant
k_{cat}	Turnover number
V_{max}	Maximum velocity of the reaction
$K_{M_{Acet}}$	Michaelis–Menten constant for acetyl-CoA
$K_{M_{M\ al}}$	Michaelis–Menten constant for malonyl-CoA
$K_{M_{NADPH}}$	Michaelis–Menten constant for NADPH
$K_{I_{Acet}}$	Inhibitor constant for acetyl-CoA
$K_{I_{M\ al}}$	Inhibitor constant for malonyl-CoA
Acet	Acetyl-CoA
Mal	Malonyl-CoA

Bioscience Reports (2023) **43** BSR20222496
https://doi.org/10.1042/BSR20222496

Abbreviations

ACC, acetyl-CoA carboxylase; ACP, acyl carrier protein; ADP, adenosine diphosphate; ATP, adenosine triphosphate; BAT, brown adipose tissue; ELOVL, elongation of very long-chain fatty acid; ER, endoplasmic reticulum; FA, fatty acid; FADNS, fatty acid *de novo* synthesis; FAS, fatty acid synthase; HCD, high carbohydrates diet; HUFA, highly unsaturated fatty acid; LC/MS/MS, liquid chromatography/mass spectrometry/mass spectrometry; LCFA, long-chain fatty acid; LCSFA, long-chain-saturated fatty acid; MS, mass spectrometry; MUFA, monounsaturated fatty acid; NADPH, nicotinamide adenine dinucleotide; ODE, ordinary differential equations; PPARα, peroxisome proliferator-activated receptor α; PUFA, polyunsaturated fatty acid; RF-MS, RapidFire Mass Spectrometry; SCD, stearoyl-CoA desaturase; SFA, saturated fatty acid; ULCFA, ultra-long-chain fatty acid; USFA, unsaturated fatty acid; VLCFA, very long-chain fatty acid; WAT, white adipose tissue.

References

1 Heil, C.S., Wehrheim, S.S., Paithankar, K.S. and Grininger, M. (2019) Fatty acid biosynthesis: chain-length regulation and control. *Chem. Bio. Chem.* **20**, 2298–2321, ISSN 14397633, https://doi.org/10.1002/cbic.201800809
2 Paiva, P., Medina, F.E., Viegas, M., Ferreira, P., Neves, R.P.P., Sousa, J.P.M. et al. (2021) Animal fatty acid synthase: a chemical nanofactory. *Chem. Rev.* **121**, 9502–9553, https://doi.org/10.1021/acs.chemrev.1c00147
3 van Meer, G., Voelker, D.R. and Feigenson, G.W. (2008) Membrane lipids: where they are and how they behave. *Nat. Rev. Mol. Cell Biol.* **9**, 112–124, https://doi.org/10.1038/nrm2330
4 Olzmann, J.A. and Carvalho, P. (2018) Dynamics and functions of lipid droplets. *Nat. Rev. Mol. Cell Biol.* **20**, 137–155, https://doi.org/10.1038/s41580-018-0085-z
5 Mashima, T., Seimiya, H. and Tsuruo, T. (2009) De novo fatty-acid synthesis and related pathways as molecular targets for cancer therapy. *Br. J. Cancer* **100**, 1369–1372, https://doi.org/10.1038/sj.bjc.6605007
6 Kuhajda, F.P. (2000) Fatty-acid synthase and human cancer: new perspectives on its role in tumor biology. *Nutrition* **16**, 202–208, https://doi.org/10.1016/S0899-9007(99)00266-X
7 Gentile, C.L. and Pagliassotti, M.J. (2008) The role of fatty acids in the development and progression of nonalcoholic fatty liver disease. *J. Nutr. Biochem.* **19**, 567–576, https://doi.org/10.1016/j.jnutbio.2007.10.001
8 Shetty, S. and Kumari, S. (2021) Fatty acids and their role in type-2 diabetes (Review). *Exp. Ther. Med.* **22**, 1–6, ISSN 1792-0981, https://doi.org/10.3892/etm.2021.10138
9 Tucci, S., Behringer, S. and Spiekerkoetter, U. (2015) De novo fatty acid biosynthesis and elongation in very long-chain acyl-CoA dehydrogenase-deficient mice supplemented with odd or even medium-chain fatty acids. *FEBS J.* **282**, 4242–4253, ISSN 17424658, https://doi.org/10.1111/febs.13418
10 Martines, A.-C.C.M.F., van Eunen, K., Reijngoud, D.J. and Bakker, B.M. (2017) The promiscuous enzyme medium-chain 3-keto-acyl-CoA thiolase triggers a vicious cycle in fatty-acid beta-oxidation. *PLoS Comput. Biol.* **13**, e1005461, ISSN 15537358, https://doi.org/10.1371/journal.pcbi.1005461
11 Voit, E.O. (2017) The best models of metabolism. *WIREs Systems Biol. Med.* **9**, https://doi.org/10.1002/wsbm.1391
12 Kim, O.D., Rocha, M. and Maia, P. (2018) A review of dynamic modeling approaches and their application in computational strain optimization for metabolic engineering. *Front. Microbiol.* **9**, https://doi.org/10.3389/fmicb.2018.01690
13 Johnson, C.H., Ivanisevic, J. and Siuzdak, G. (2016) Metabolomics: beyond biomarkers and towards mechanisms. *Nat. Rev. Mol. Cell Biol.* **17**, 451–459, https://doi.org/10.1038/nrm.2016.25
14 Gombert, A.K. and Nielsen, J. (2000) Mathematical modelling of metabolism. *Curr. Opin. Biotechnol.* **11**, 180–186, https://doi.org/10.1016/S0958-1669(00)00079-3
15 Fischer, H.P. (2008) Mathematical modeling of complex biological systems: from parts lists to understanding systems behavior. *Alcohol Res. Health* **31**, 49–59
16 Voit, E.O. (2012) *A First Course in Systems Biology.*, Garland Science, Taylor & Francis distributor, New York
17 Cobelli, C., Mari, A.J., Toffolo, G., Cherrington, A.D. and McGuinness, O.P. (1987) Dynamic control of insulin on glucose kinetics: tracer experiment design and time-varying interpretative models. *IFAC Proc. Vol.* **20**, 25–30, ISSN 14746670, https://doi.org/10.1016/S1474-6670(17)55237-4
18 Kohn, M.C. (1983) Computer simulation of metabolism in palmitate-perfused rat heart. III. Sensitivity analysis. *Ann. Biomed. Eng.* **11**, 533–549, ISSN 00906964, https://doi.org/10.1007/BF02364083
19 Schulz, H. (1991) Beta oxidation of fatty acids. *Biochim. Biophys. Acta* **1081**, 109–120, ISSN 0005-2760, https://doi.org/10.1016/0005-2760(91)90015-A
20 Wanders, R.J.A., Ruiter, J.P.N., IJlst, L., Waterham, H.R. and Houten, S.M. (2010) The enzymology of mitochondrial fatty acid beta-oxidation and its application to follow-up analysis of positive neonatal screening results. *J. Inherit. Metab. Dis.* **33**, 479–494, https://doi.org/10.1007/s10545-010-9104-8
21 Houten, S.M., Violante, S., Ventura, F.V. and Wanders, R.J.A. (2016) The biochemistry and physiology of mitochondrial fatty acid β-oxidation and its genetic disorders. *Annu. Rev. Physiol.* **78**, 23–44, https://doi.org/10.1146/annurev-physiol-021115-105045
22 Vishwanath, V.A. (2016) Fatty acid beta-oxidation disorders: a brief review. *Ann. Neurosci.* **23**, 51–55, https://doi.org/10.1159/000443556
23 Modre-Osprian, R., Osprian, I., Tilg, B., Schreier, G., Weinberger, K.M. and Graber, A. (2009) Dynamic simulations on the mitochondrial fatty acid beta-oxidation network. *BMC Syst. Biol.* **3**, 1–15, ISSN 17520509, https://doi.org/10.1186/1752-0509-3-2
24 van Eunen, K., Simons, S.M.J., Gerding, A., Bleeker, A., den Besten, G., Touw, C.M.L. et al. (2013) Biochemical competition makes fatty-acid β-oxidation vulnerable to substrate overload. *PLoS Comput. Biol.* **9**, e1003186, ISSN 15537358, https://doi.org/10.1371/journal.pcbi.1003186

25 Abegaz, F., Martines, A.-C.M.F., Vieira Lara, M.A., Morales, M.R., Reijngoud, D.J., Wit, E.C. et al. (2021) Bistability in fatty-acid oxidation resulting from substrate inhibition. *PLoS Comput. Biol.* **17**, e1009259, ISSN 15537358, https://doi.org/10.1371/journal.pcbi.1009259
26 Feist, A.M. and Palsson, B.O. (2010) The biomass objective function. *Curr. Opin. Microbiol.* **13**, 344–349, https://doi.org/10.1016/j.mib.2010.03.003
27 Cleland, W.W. (1963) The kinetics of enzyme-catalyzed reactions with two or more substrates or products. II. Inhibition: nomenclature and theory. *Biochim. Biophys. Acta* **67**, 173–187, ISSN 00063002, https://doi.org/10.1016/0926-6569(63)90226-8
28 Rohwer, J.M., Hanekom, A.J., Crous, C., Snoep, J.L. and Hofmeyr, J.H.S. (2006) Evaluation of a simplified generic bi-substrate rate equation for computational systems biology. *IEE Proc.: Systems Biol.* **153**, 338–341, ISSN 17412471, https://doi.org/10.1049/ip-syb:20060026
29 Saa, P.A. and Nielsen, L.K. (2017) Formulation, construction and analysis of kinetic models of metabolism: a review of modelling frameworks. *Biotechnol. Adv.* **35**, 981–1003, ISSN 0734-9750. Metabolic engineering frontiers emerging with advanced tools and methodologies https://www.sciencedirect.com/science/article/pii/S0734975017301167, https://doi.org/10.1016/j.biotechadv.2017.09.005
30 Rodriguez, J.M.G., Hux, N.P., Philips, S.J. and Towns, M.H. (2019) Michaelis-Menten graphs, Lineweaver-Burk plots, and reaction schemes: investigating introductory biochemistry students' conceptions of representations in enzyme kinetics. *J. Chem. Educ.* **96**, 1833–1845, ISSN 19381328, https://doi.org/10.1021/acs.jchemed.9b00396
31 Saboury, A.A. (2009) Enzyme inhibition and activation: a general theory. *J. Iran. Chem. Soc.* **6**, 219–229, https://doi.org/10.1007/BF03245829
32 Waldrop, G.L. (2009) A qualitative approach to enzyme inhibition. *Biochem. Mol. Biol. Educ.* **37**, 11–15, https://doi.org/10.1002/bmb.20243
33 Rittner, A., Paithankar, K.S., Huu, K.V. and Grininger, M. (2018) Characterization of the polyspecific transferase of murine type i fatty acid synthase (FAS) and implications for polyketide synthase (PKS) engineering. *ACS Chem. Biol.* **13**, 723–732, ISSN 15548937, https://doi.org/10.1021/acschembio.7b00718
34 Cox, B.G. and Hammes, G.G. (1983) Steady-state kinetic study of fatty acid synthase from chicken liver. *PNAS* **80**, 4233–4237, ISSN 00278424, https://doi.org/10.1073/pnas.80.14.4233
35 Liebermeister, W. and Klipp, E. (2006) Bringing metabolic networks to life: convenience rate law and thermodynamic constraints. *Theor. Biol. Med. Model.* **3**, 1–13, ISSN 17424682, https://doi.org/10.1186/1742-4682-3-41
36 Michaelis, L., Menten, M.L. et al. (1913) Die kinetik der invertinwirkung. *Biochem. Z.* **49**, 352, https://path.upmc.edu/divisions/chp/pdf/michaelis-menten_kinetik.pdf
37 Rohwer, J., Hanekom, A. and Hofmeyr, J.-H. (2007) A universal rate equation for systems biology. *Proceed. 2nd Intern. ESCEC Symp.* 175–187, https://www.beilstein-institut.de/download/691/rohwer_1.pdf
38 King, E.L. and Altman, C. (1956) A schematic method of deriving the rate laws for enzyme-catalyzed reactions. *J. Phys. Chem.* **60**, 1375–1378, ISSN 00223654, https://doi.org/10.1021/j150544a010
39 Happel, J. and Sellers, P.H. (1995) New perspective on the kinetics of enzyme catalysis. *J. Phys. Chem.* **99**, 6595–6600, ISSN 00223654, https://doi.org/10.1021/j100017a048
40 Happel, J. and Sellers, P.H. (1992) Systemization for the King-Altman-Hill diagram method in chemical kinetics. *J. Phys. Chem.* **96**, 2593–2597, ISSN 00223654, https://doi.org/10.1021/j100185a037
41 Ulusu, N.N. (2015) Evolution of enzyme kinetic mechanisms. *J. Mol. Evol.* **80**, 251–257, https://doi.org/10.1007/s00239-015-9681-0
42 van Aalst, M., Ebenhöh, O. and Matuszyńska, A. (2021) Constructing and analysing dynamic models with modelbase v1.2.3: a software update. *BMC Bioinformatics* **22**, 1–15, ISSN 14712105, https://doi.org/10.1186/s12859-021-04122-7
43 Hoops, S., Gauges, R., Lee, C., Pahle, J., Simus, N., Singhal, M. et al. (2006) COPASI - a COmplex PAthway SImulator. *Bioinformatics* **22**, 3067–3074, ISSN 13674803, https://doi.org/10.1093/bioinformatics/btl485
44 Olivier, B.G., Rohwer, J.M. and Hofmeyr, J.H.S. (2005) Modelling cellular systems with PySCeS. *Bioinformatics* **21**, 560–561, ISSN 13674803, https://doi.org/10.1093/bioinformatics/bti046
45 Marcoline, F.V., Furth, J., Nayak, S., Grabe, M. and Macey, R.I. (2022) Berkeley Madonna Version 10-A simulation package for solving mathematical models. *CPT. Pharmacometrics Syst. Pharmacol.* **11**, 290–301, ISSN 21638306, https://doi.org/10.1002/psp4.12757
46 van Eunen, K., Simons, S.M.J., Gerding, A., Bleeker, A., den Besten, G., Touw, C.M.L. et al. (2013) Biochemical competition makes fatty-acid β-oxidation vulnerable to substrate overload. *PLoS Comput. Biol.* **9**, e1003186, https://doi.org/10.1371/journal.pcbi.1003186
47 Bordbar, A., McCloskey, D., Zielinski, D.C., Sonnenschein, N., Jamshidi, N. and Palsson, B.O. (2015) Personalized whole-cell kinetic models of metabolism for discovery in genomics and pharmacodynamics. *Cell Systems* **1**, 283–292, ISSN 24054712, https://doi.org/10.1016/j.cels.2015.10.003
48 Haanstra, J.R., Gerding, A., Dolga, A.M., Sorgdrager, F.J.H., Buist-Homan, M., Du Toit, F. et al. (2017) Targeting pathogen metabolism without collateral damage to the host. *Sci. Rep.* **7**, 1–15, ISSN 20452322, https://doi.org/10.1038/srep40406
49 Santos, C.R. and Schulze, A. (2012) Lipid metabolism in cancer. *FEBS J.* **279**, 2610–2623, https://doi.org/10.1111/j.1742-4658.2012.08644.x
50 de Cedrón, M.G. and de Molina, A.R. (2020) Precision nutrition to target lipid metabolism alterations in cancer. In *Precision Medicine for Investigators, Practitioners and Providers* (Faintuch, J. and Faintuch, S., eds), pp. 291–299, Academic Press, London, https://doi.org/10.1016/B978-0-12-819178-1.00028-9
51 Ookhtens, M., Kannan, R., Lyon, I. and Baker, N. (1984) Liver and adipose tissue contributions to newly formed fatty acids in an ascites tumor. *Am. J. Physiol.* **247**, R146–R153, https://doi.org/10.1152/ajpregu.1984.247.1.R146
52 Menendez, J.A. and Lupu, R. (2007) Fatty acid synthase and the lipogenic phenotype in cancer pathogenesis. *Nat. Rev. Cancer* **7**, 763–777, https://doi.org/10.1038/nrc2222
53 Fhu, C.W. and Ali, A. (2020) Fatty acid synthase: an emerging target in cancer. *Molecules* **25**, 3935, https://doi.org/10.3390/molecules25173935
54 Lelliott, C. and Vidal-Puig, A.J. (2004) Lipotoxicity, an imbalance between lipogenesis de novo and fatty acid oxidation. *Int. J. Obes.* **28**, S22–S28, Nature Publishing Group, https://doi.org/10.1038/sj.ijo.0802854

55 Hansen, H.J.M., Carey, E.M. and Dils, R. (1970) Fatty acid biosynthesis VII. Substrate control of chain-length of products synthesised by rat liver fatty acid synthetase. *Biochim. Biophys. Acta* **210**, 400–410, ISSN 00052760, https://doi.org/10.1016/0005-2760(70)90035-4
56 Carey, E.M., Dils, R. and Hansen., H.J. (1970) Short communications. Chain-length specificity for termination of atty acid biosynthesis by fatty acid synthetase complexes from lactating rabbit mamary gland and rat liver. *Biochem. J.* **117**, 633–635, ISSN 02646021, https://doi.org/10.1042/bj1170633
57 Topolska, M., Martínez-montañés, F. and Ejsing, C.S. (2020) A simple and direct assay for monitoring fatty acid synthase activity and product-specificity by high-resolution mass spectrometry. *Biomolecules* **10**, 118, ISSN 2218273X, https://doi.org/10.3390/biom10010118
58 Brownsey, R.W., Boone, A.N., Elliott, J.E., Kulpa, J.E. and Lee, W.M. (2006) Regulation of acetyl-CoA carboxylase. *Biochem. Soc. Trans.* **34**, 223–227, https://doi.org/10.1042/BST0340223
59 Wang, Y., Yu, W., Li, S., Guo, D., He, J. and Wang, Y. (2022) Acetyl-CoA carboxylases and diseases. *Front. Oncol.* **12**, https://doi.org/10.3389/fonc.2022.836058
60 Wakil, S.J. and Abu-Elheiga, L.A. (2009) Fatty acid metabolism: target for metabolic syndrome. *J. Lipid Res.* **50**, S138–S143, https://doi.org/10.1194/jlr.R800079-JLR200
61 Jayakumar, A., Tai, M.-H., Huang, W.-Y., Al-Feel, W., Hsu, M., Abu-Elheiga, L. et al. (1995) Human fatty acid synthase: properties and molecular cloning. *Proc. Natl. Acad. Sci. U.S.A.* **92**, 8695–8699, https://doi.org/10.1073/pnas.92.19.8695
62 Fullerton, M.D., Galic, S., Marcinko, K., Sikkema, S., Pulinilkunnil, T., Chen, Z.P. et al. (2013) Single phosphorylation sites in Acc1 and Acc2 regulate lipid homeostasis and the insulin-sensitizing effects of metformin. *Nat. Med.* **19**, 1649–1654, ISSN 10788956, https://doi.org/10.1038/nm.3372
63 Wright, T.C., Cant, J.P., Brenna, J.T. and McBride, B.W. (2006) Acetyl CoA carboxylase shares control of fatty acid synthesis with fatty acid synthase in bovine mammary homogenate. *J. Dairy Sci.* **89**, 2552–2558, ISSN 00220302, https://doi.org/10.3168/jds.S0022-0302(06)72331-1
64 Abu-Elheiga, L., Almarza-Ortega, D.B., Baldini, A. and Wakil., S.J. (1997) Human acetyl-CoA carboxylase 2. Molecular cloning, characterization, chromosomal mapping, and evidence for two isoforms. *J. Biol. Chem.* **272**, 10669–10677, ISSN 00219258, https://doi.org/10.1074/jbc.272.16.10669
65 Abu-Elheiga, L., Brinkley, W.R., Zhong, L., Chirala, S.S., Woldegiorgis, G. and Wakil, S.J. (2000) The subcellular localization of acetyl-CoA carboxylase 2. *PNAS* **97**, 1444–1449, ISSN 00278424, https://doi.org/10.1073/pnas.97.4.1444
66 Cheng, D., Chu, C.H., Chen, L., Feder, J.N., Mintier, G.A., Wu, Y. et al. (2007) Expression, purification, and characterization of human and rat acetyl cfenzyme A carboxylase (ACC) isozymes. *Protein Expr. Purif.* **51**, 11–21, ISSN 10465928, https://doi.org/10.1016/j.pep.2006.06.005
67 Kaushik, V.K., Kavana, M., Volz, J.M., Weldon, S.C., Hanrahan, S., Xu, J. et al. (2009) Characterization of recombinant human acetyl-CoA carboxylase-2 steady-state kinetics. *Biochim. Biophys. Acta* **1794**, 961–967, https://doi.org/10.1016/j.bbapap.2009.02.004
68 Trumble, G.E., Smith, M.A. and Winder, W.W. (1995) Purification and characterization of rat skeletal muscle acetyl-CoA carboxylase. *Eur. J. Biochem.* **231**, 192–198, https://doi.org/10.1111/j.1432-1033.1995.tb20686.x
69 Abu-Elheiga, L., Matzuk, M.M., Abo-Hashema, K.A.H. and Wakil, S.J. (2001) Continuous fatty acid oxidation and reduced fat storage in mice lacking acetyl-coa carboxylase 2. *Science* **291**, 2613–2616, ISSN 00368075, https://doi.org/10.1126/science.1056843
70 Mao, J., DeMayo, F.J., Li, H., Abu-Elheiga, L., Gu, Z., Shaikenov, T.E. et al. (2006) Liver-specific deletion of acetyl-CoA carboxylase 1 reduces hepatic triglyceride accumulation without affecting glucose homeostasis. *Proc. Natl. Acad. Sci. U.S.A.* **103**, 8552–8557, https://doi.org/10.1073/pnas.0603115103
71 Savage, D.B., Petersen, K.F. and Shulman, G.I. (2007) Disordered lipid metabolism and the pathogenesis of insulin resistance. *Physiol. Rev.* **87**, 507–520, https://doi.org/10.1152/physrev.00024.2006
72 Abu-Elheiga, L., Oh, W., Kordari, P. and Wakil, S.J. (2003) Acetyl-CoA carboxylase 2 mutant mice are protected against obesity and diabetes induced by high-fat/high-carbohydrate diets. *PNAS* **100**, 10207–10212, ISSN 00278424, https://doi.org/10.1073/pnas.1733877100
73 Wakil, S.J. (1970) Lipid Metabolism. 1–9, ed. Wakil, SJ
74 Numa, S. and Tanabe, T. (1984) Chapter 1 Acetyl-coenzyme A carboxylase and its regulation. *New Compr. Biochem.* **7**, 1–27, ISSN 01677306, https://doi.org/10.1016/S0167-7306(08)60119-2
75 Ogiwara, H., Tanabe, T., Nikawa, J.-i. and Numa, S. (1978) Inhibition of rat-liver acetyl-coenzyme-A carboxylase by palmitoyl-coenzyme A: formation of equimolar enzyme-inhibitor complex. *Eur. J. Biochem.* **89**, 33–41, ISSN 14321033, https://doi.org/10.1111/j.1432-1033.1978.tb20893.x
76 Moule, S.K., Edgell, N.J., Borthwick, A.C. and Denton, R.M. (1992) Coenzyme A is a potent inhibitor of acetyl-CoA carboxylase from rat epididymal fat-pads. *Biochem. J.* **283**, 35–38, ISSN 02646021, https://doi.org/10.1042/bj2830035
77 Munday, M.R. and Hemingway, C.J. (1999) The regulation of acetyl-CoA carboxylase - a potential target for the action of hypolipidemic agents. *Adv. Enzyme. Regul.* **39**, 205–234, https://doi.org/10.1016/S0065-2571(98)00016-8
78 Munday, M.R. (2002) Regulation of mammalian acetyl-CoA carboxylase. *Biochem. Soc. Trans.* **30**, 1059–1064, https://doi.org/10.1042/bst0301059
79 Goodridge, A.G. (1972) Regulation of the activity of acetyl coenzyme A carboxylase by palmitoyl coenzyme A and citrate. *J. Biol. Chem.* **247**, 6946–6952, ISSN 00219258, https://doi.org/10.1016/S0021-9258(19)44677-2
80 Tong, L. (2012) Structure and function of biotin-dependent carboxylases. *Cell. Mol. Life Sci.* **70**, 863–891, https://doi.org/10.1007/s00018-012-1096-0
81 Hashimoto, T., Isano, H., Iritani, N. and Numa, S. (1971) Liver acetyl-coenzyme-A carboxylase: studies on kynurenate inhibition, isotope exchange and interaction of the uncarboxylated enzyme with citrate. *Eur. J. Biochem.* **24**, 128–139, ISSN 14321033, https://doi.org/10.1111/j.1432-1033.1971.tb19663.x
82 Beaty, N.B. and Lane, M.D. (1982) Acetyl coenzyme A carboxylase. Rapid purification of the chick liver enzyme and steady state kinetic analysis of the carboxylase-catalyzed reaction. *J. Biol. Chem.* **257**, 924–929, ISSN 00219258, https://doi.org/10.1016/S0021-9258(19)68288-8
83 Tanabe, T., Nakanishi, S., Hashimoto, T., Ogiwara, H., Nikawa, J.-i. and Numa, S. (1981) [1] Acetyl-CoA carboxylase from rat liver. *Methods Enzymol.* **71**, 5–16, Elsevier, https://doi.org/10.1016/0076-6879(81)71003-6

84 Wakil, S.J., Pugh, E.L. and Sauer, F. (1964) The mechanism of fatty acid synthesis. *PNAS* **52**, 106, https://doi.org/10.1073/pnas.52.1.106
85 Majerus, P.W., Alberts, A.W. and Vagelos, P.R. (1964) The acyl carrier protein of fatty acid synthesis: purification. *Proc. Natl. Acad. Sci. U.S.A.* **51**, 1231–1238, ISSN 00278424, https://doi.org/10.1073/pnas.51.6.1231
86 Wakil, S.J. (1989) Fatty acid synthase, a proficient multifunctional enzyme. *Biochemistry* **28**, 4523–4530, ISSN 15204995, https://doi.org/10.1021/bi00437a001
87 Chakravarty, B., Gu, Z., Chirala, S.S., Wakil, S.J. and Quiocho, F.A. (2004) Human fatty acid synthase: structure and substrate selectivity of the thioesterase domain. *PNAS* **101**, 15567–15572, ISSN 00278424, https://doi.org/10.1073/pnas.0406901101
88 Katiyar, S.S., Cleland, W.W. and Porter, J.W. (1975) Fatty acid synthetase. A steady state kinetic analysis of the reaction catalyzed by the enzyme from pigeon liver. *J. Biol. Chem.* **250**, 2709–2727, ISSN 00219258, https://doi.org/10.1016/S0021-9258(19)41660-8
89 Rangan, V.S. and Smith, S. (1997) Alteration of the substrate specificity of the malonyl-CoA/acetyl- CoA:acyl carrier protein S-acyltransferase domain of the multifunctional fatty acid synthase by mutation of a single arginine residue. *J. Biol. Chem.* **272**, 11975–11978, ISSN 00219258, https://doi.org/10.1074/jbc.272.18.11975
90 Rittner, A., Paithankar, K.S., Himmler, A. and Grininger, M. (2020) Type I fatty acid synthase trapped in the octanoyl-bound state. *Protein Sci.* **29**, 589–605, ISSN 1469896X, https://doi.org/10.1002/pro.3797
91 Aprahamian, S.A., Arslanian, M.J. and Wakil, S.J. (1982) Comparative studies on the kinetic parameters and product analyses of chicken and rat liver and yeast fatty acid synthetase. *Comp. Biochem. Physiol. B* **71**, 577–582, ISSN 03050491, https://doi.org/10.1016/0305-0491(82)90465-5
92 Carlisle-Moore, L., Gordon, C.R., Machutta, C.A., Miller, W.T. and Tonge, P.J. (2005) Substrate recognition by the human fatty-acid synthase. *J. Biol. Chem.* **280**, 42612–42618, ISSN 00219258, https://doi.org/10.1074/jbc.M507082200
93 Ohashi, K., Otsuka, H. and Seyama, Y. (1985) Assay of fatty acid synthetase by mass fragmentography using [13c]malonyl-CoA. *J. Biochem. (Tokyo)* **97**, 867–875, ISSN 0021924X, https://doi.org/10.1093/oxfordjournals.jbchem.a135128
94 Connor, W.E. (2000) Importance of n-3 fatty acids in health and disease. *Am. J. Clin. Nutr.* **71**, 171S–175S, Oxford University Press, https://doi.org/10.1093/ajcn/71.1.171S
95 Nagy, K. and Tiuca, I.-D. (2017) Importance of fatty acids in physiopathology of human body. *Fatty Acids*, IntechOpen, London, https://doi.org/10.5772/67407
96 Ohno, Y., Suto, S., Yamanaka, M., Mizutani, Y., Mitsutake, S., Igarashi, Y. et al. (2010) ELOVL1 production of C24 acyl-CoAs is linked to C24 sphingolipid synthesis. *PNAS* **107**, 18439–18444, ISSN 00278424, https://doi.org/10.1073/pnas.1005572107
97 Nakamura, M.T. and Nara, T.Y. (2004) Structure, function, and dietary regulation of $\Delta 6$, $\Delta 5$, and $\Delta 9$ desaturases. *Annu. Rev. Nutr.* **24**, 345–376, https://doi.org/10.1146/annurev.nutr.24.121803.063211
98 Yang, X., Sheng, W., Sun, G.Y. and Lee, J.C.-M. (2011) Effects of fatty acid unsaturation numbers on membrane fluidity and α-secretase-dependent amyloid precursor protein processing. *Neurochem. Int.* **58**, 321–329, ISSN 01970186, https://doi.org/10.1016/j.neuint.2010.12.004
99 Guillou, H., Zadravec, D., Martin, P.G.P. and Jacobsson, A. (2010) The key roles of elongases and desaturases in mammalian fatty acid metabolism: insights from transgenic mice. *Prog. Lipid Res.* **49**, 186–199, https://doi.org/10.1016/j.plipres.2009.12.002
100 Kihara, A. (2012) Very long-chain fatty acids: elongation, physiology and related disorders. *J. Biochem.* **152**, 387–395, https://doi.org/10.1093/jb/mvs105
101 Deák, F., Anderson, R.E., Fessler, J.L. and Sherry, D.M. (2019) Novel cellular functions of very long chain-fatty acids: insight from ELOVL4 mutations. *Front. Cell. Neurosci.* **13**, https://doi.org/10.3389/fncel.2019.00428
102 Park, W.J. (2018) The biochemistry and regulation of fatty acid desaturases in animals. In *Polyunsaturated Fatty Acid Metabolism* (Burdge, G.C., ed.), pp. 87–100, AOCS Press, Urbana, IL 61802-6996, USA, https://doi.org/10.1016/B978-0-12-811230-4.00005-3
103 Jump, D.B. (2009) Mammalian fatty acid elongases. *Methods Mol. Biol.* **579**, 375–389, ISSN 10643745, https://doi.org/10.1007/978-1-60761-322-0˙19
104 Jakobsson, A., Westerberg, R. and Jacobsson, A. (2006) Fatty acid elongases in mammals: their regulation and roles in metabolism. *Prog. Lipid Res.* **45**, 237–249, https://doi.org/10.1016/j.plipres.2006.01.004
105 Green, C.D., Ozguden-Akkoc, C.G., Wang, Y., Jump, D.B. and Olson, L.K. (2010) Role of fatty acid elongases in determination of de novo synthesized monounsaturated fatty acid species [s]. *J. Lipid Res.* **51**, 1871–1877, https://doi.org/10.1194/jlr.M004747
106 Sassa, T., Ohno, Y., Suzuki, S., Nomura, T., Nishioka, C., Kashiwagi, T. et al. (2013) Impaired epidermal permeability barrier in mice lacking Elovl1, the gene responsible for very-long-chain fatty acid production. *Mol. Cell. Biol.* **33**, 2787–2796, ISSN 0270-7306, https://doi.org/10.1128/MCB.00192-13
107 Nugteren, D.H. (1965) The enzymic chain elongation of fatty acids by rat-liver microsomes. *Biochim. Biophys. Acta* **106**, 280–290, ISSN 00052760, https://doi.org/10.1016/0005-2760(65)90036-6
108 Kugi, M., Yoshida, S. and Takeshita, M. (1990) Characterization of fatty acid elongation system in porcine neutrophil microsomes. *Biochim. Biophys. Acta* **1043**, 83–90, ISSN 00052760, https://doi.org/10.1016/0005-2760(90)90113-C
109 Naganuma, T., Sato, Y., Sassa, T., Ohno, Y. and Kihara, A. (2011) Biochemical characterization of the very long-chain fatty acid elongase ELOVL7. *FEBS Lett.* **585**, 3337–3341, ISSN 00145793, https://doi.org/10.1016/j.febslet.2011.09.024
110 Naganuma, T. and Kihara, A. (2014) Two modes of regulation of the fatty acid elongase ELOVL6 by the 3-ketoacyl-CoA reductase KAR in the fatty acid elongation cycle. *PloS ONE* **9**, e101823, ISSN 19326203, https://doi.org/10.1371/journal.pone.0101823
111 Matsuzaka, T., Shimano, H., Yahagi, N., Yoshikawa, T., Amemiya-Kudo, M., Hasty, A.H. et al. (2002) Cloning and characterization of a mammalian fatty acyl-CoA elongase as a lipogenic enzyme regulated by SREBPs. *J. Lipid Res.* **43**, 911–920, ISSN 00222275, https://doi.org/10.1016/S0022-2275(20)30465-X
112 Harroun, S.G., Lauzon, D., Ebert, M.C.C.J.C., Desrosiers, A., Wang, X. and Vallée-Bélisle, A. (2022) Monitoring protein conformational changes using fluorescent nanoantennas. *Nat. Methods* **19**, 71–80, ISSN 15487105, https://doi.org/10.1038/s41592-021-01355-5

113 Cook, H.W. and McMaster, C.R. (2002) Chapter 7 fatty acid desaturation and chain elongation in eukaryotes. *New Compr. Biochem.* **36**, 181–204, ISSN 01677306, https://doi.org/10.1016/S0167-7306(02)36009-5
114 Ntambi, J.M. (1999) Regulation of stearoyl-CoA desaturase by polyunsaturated fatty acids and cholesterol. *J. Lipid Res.* **40**, 1549–1558, https://doi.org/10.1016/S0022-2275(20)33401-5
115 Cho, H.P., Nakamura, M.T. and Clarke, S.D. (1999) Cloning, expression, and nutritional regulation of the mammalian △-6 desaturase. *J. Biol. Chem.* **274**, 471–477, ISSN 00219258, https://doi.org/10.1074/jbc.274.1.471
116 Cho, H.P., Nakamura, M. and Clarke, S.D. (1999) Cloning, expression, and fatty acid regulation of the human △-5 desaturase. *J. Biol. Chem.* **274**, 37335–37339, ISSN 00219258, https://doi.org/10.1074/jbc.274.52.37335
117 Ntambi, J. (2004) Regulation of stearoyl-CoA desaturases and role in metabolism. *Prog. Lipid Res.* **43**, 91–104, https://doi.org/10.1016/S0163-7827(03)00039-0
118 Ntambi, J.M. and Miyazaki, M. (2003) Recent insights into stearoyl-CoA desaturase-1. *Curr. Opin. Lipidol.* **14**, 255–261, https://doi.org/10.1097/00041433-200306000-00005
119 Flowers, M.T. and Ntambi, J.M. (2008) Role of stearoyl-coenzyme a desaturase in regulating lipid metabolism. *Curr. Opin. Lipidol.* **19**, 248–256, https://doi.org/10.1097/MOL.0b013e3282f9b54d
120 Ntambi, J.M., Miyazaki, M., Stoehr, J.P., Lan, H., Kendziorski, C.M., Yandell, B.S. et al. (2002) Loss of stearoyl-CoA desaturase-1 function protects mice against adiposity. *PNAS* **99**, 11482–11486, ISSN 00278424, https://doi.org/10.1073/pnas.132384699
121 Miyazaki, M., Sampath, H., Liu, X., Flowers, M.T., Chu, K., Dobrzyn, A. et al. (2009) Stearoyl-CoA desaturase-1 deficiency attenuates obesity and insulin resistance in leptin-resistant obese mice. *Biochem. Biophys. Res. Commun.* **380**, 818–822, ISSN 0006291X, https://doi.org/10.1016/j.bbrc.2009.01.183
122 Soulard, P., McLaughlin, M., Stevens, J., Connolly, B., Coli, R., Wang, L. et al. (2008) Development of a high-throughput screening assay for stearoyl-CoA desaturase using rat liver microsomes, deuterium labeled stearoyl-CoA and mass spectrometry. *Anal. Chim. Acta* **627**, 105–111, ISSN 00032670, https://doi.org/10.1016/j.aca.2008.04.017
123 McDonald, T.M. and Kinsella, J.E. (1973) Stearyl-CoA desaturase of bovine mammary microsomes. *Arch. Biochem. Biophys.* **156**, 223–231, ISSN 10960384, https://doi.org/10.1016/0003-9861(73)90360-3
124 Strittmatter, P. and Enoch, H.G. (1978) Purification of stearyl-CoA desaturase from liver. *Methods Enzymol.* **52**, 188–193, ISSN 15577988, https://doi.org/10.1016/S0076-6879(78)52020-X
125 Ge, L., Gordon, J.S., Hsuan, C., Stenn, K. and Prouty, S.M. (2003) Identification of the δ-6 desaturase of human sebaceous glands: expression and enzyme activity. *J. Invest. Dermatol.* **120**, 707–714, ISSN 0022202X, https://doi.org/10.1046/j.1523-1747.2003.12123.x
126 Okayasu, T., Nagao, M., Ishibashi, T. and Imai, Y. (1981) Purification and partial characterization of linoleoyl-coa desaturase from rat liver microsomes. *Arch. Biochem. Biophys.* **206**, 21–28, https://doi.org/10.1016/0003-9861(81)90061-8
127 Rodriguez, A., Sarda, P., Nessmann, C., Boulot, P., Leger, C.L. and Descomps, B. (1998) △6- and △5-desaturase activities in the human fetal liver: kinetic aspects. *J. Lipid Res.* **39**, 1825–1832, ISSN 00222275, https://doi.org/10.1016/S0022-2275(20)32170-2
128 Irazú, C.E., González-Rodríguez, S. and Brenner, R.R. (1993) △5 Desaturase activity in rat kidney microsomes. *Mol. Cell. Biochem.* **129**, 31–37, ISSN 03008177, https://doi.org/10.1007/BF00926573
129 Natesan, V. and Kim, S.-J. (2021) Lipid metabolism, disorders and therapeutic drugs–review. *Biomol. Ther.* **29**, 596, https://doi.org/10.4062/biomolther.2021.122
130 Hems, D.A., Rath, E.A. and Verrinder, T.R. (1975) Fatty acid synthesis in liver and adipose tissue of normal and genetically obese (ob/ob) mice during the 24-hour cycle. *Biochem. J.* **150**, 167–173, https://doi.org/10.1042/bj1500167
131 Shanmugarajah, K., Linka, N., Gräfe, K., Smits, S.H.J., Weber, A.P.M., Zeier, J. et al. (2019) ABCG1 contributes to suberin formation in Arabidopsis thaliana roots. *Sci. Rep.* **9**, 1–12, ISSN 20452322, https://doi.org/10.1038/s41598-019-47916-9
132 Jang, M., Neuzil, P., Volk, T., Manz, A. and Kleber, A. (2015) On-chip three-dimensional cell culture in phaseguides improves hepatocyte functions in vitro. *Biomicrofluidics* **9**, 34113, ISSN 19321058, https://doi.org/10.1063/1.4922863
133 Zhang, J., Li, D., Yue, X., Zhang, M., Liu, P. and Li, G. (2018) Colorimetric in situ assay of membrane-bound enzyme based on lipid bilayer inhibition of ion transport. *Theranostics* **8**, 3275–3283, ISSN 18387640, https://doi.org/10.7150/thno.25123
134 Kim, K.W., Yamane, H., Zondlo, J., Busby, J. and Wang, M. (2007) Expression, purification, and characterization of human acetyl-CoA carboxylase 2. *Protein Expr. Purif.* **53**, 16–23, ISSN 10465928, https://doi.org/10.1016/j.pep.2006.11.021
135 Tvrdik, P., Westerberg, R., Silve, S., Asadi, A., Jakobsson, A., Cannon, B. et al. (2000) Role of a new mammalian gene family in the biosynthesis of very long chain fatty acids and sphingolipids. *J. Cell Biol.* **149**, 707–717, ISSN 00219525, https://doi.org/10.1083/jcb.149.3.707
136 Sassa, T. and Kihara, A. (2014) Metabolism of very long-chain fatty acids: Genes and pathophysiology. *Biomol. Ther.* **22**, 83–92, https://doi.org/10.4062/biomolther.2014.017
137 Kitazawa, H., Miyamoto, Y., Shimamura, K., Nagumo, A. and Tokita, S. (2009) Development of a high-density assay for long-chain fatty acyl-CoA elongases. *Lipids* **44**, 765–773, https://doi.org/10.1007/s11745-009-3320-8
138 Moon, Y.A., Shah, N.A., Mohapatra, S., Warrington, J.A. and Horton, J.D. (2001) Identification of a mammalian long chain fatty acyl elongase regulated by sterol regulatory element-binding proteins. *J. Biol. Chem.* **276**, 45358–45366, ISSN 00219258, https://doi.org/10.1074/jbc.M108413200
139 Zadravec, D., Tvrdik, P., Guillou, H., Haslam, R., Kobayashi, T., Napier, J.A. et al. (2011) ELOVL2 controls the level of n-6 28:5 and 30:5 fatty acids in testis, a prerequisite for male fertility and sperm maturation in mice. *J. Lipid Res.* **52**, 245–255, ISSN 00222275, https://doi.org/10.1194/jlr.M011346
140 Matsuzaka, T. and Shimano, H. (2009) Elovl6: a new player in fatty acid metabolism and insulin sensitivity. *J. Mol. Med.* **87**, 379–384, https://doi.org/10.1007/s00109-009-0449-0
141 Matsuzaka, T., Shimano, H., Yahagi, N., Kato, T., Atsumi, A., Yamamoto, T. et al. (2007) Crucial role of a long-chain fatty acid elongase, Elovl6, in obesity-induced insulin resistance. *Nat. Med.* **13**, 1193–1202, ISSN 10788956, https://doi.org/10.1038/nm1662

142 Tamura, K., Makino, A., Hullin-Matsuda, F., Kobayashi, T., Furihata, M., Chung, S. et al. (2009) Novel lipogenic enzyme ELOVL7 is involved in prostate cancer growth through saturated long-chain fatty acid metabolism. *Cancer Res.* **69**, 8133–8140, ISSN 00085472, https://doi.org/10.1158/0008-5472.CAN-09-0775

143 Enoch, H.G., Catala, A. and Strittmatter, P. (1976) Mechanism of rat liver microsomal stearyl CoA desaturase. Studies of the substrate specificity, enzyme substrate interactions, and the function of lipid. *J. Biol. Chem.* **251**, 5095–5103, ISSN 00219258, https://doi.org/10.1016/S0021-9258(17)33223-4

144 Zheng, Y., Prouty, S.M., Harmon, A., Sundberg, J.P., Stenn, K.S. and Parimoo, S. (2001) Scd3 - a novel gene of the stearoyl-CoA desaturase family with restricted expression in skin. *Genomics* **71**, 182–191, ISSN 08887543, https://doi.org/10.1006/geno.2000.6429

145 Zhang, L., Ge, L., Parimoo, S., Stenn, K. and Prouty, S.M. (1999) Human stearoyl-CoA desaturase: alternative transcripts generated from a single gene by usage of tandem polyadenylation sites. *Biochem. J.* **340**, 255–264, ISSN 02646021, https://doi.org/10.1042/bj3400255

146 Wang, J., Yu, L., Schmidt, R.E., Su, C., Huang, X., Gould, K. et al. (2005) Characterization of HSCD5, a novel human stearoyl-CoA desaturase unique to primates. *Biochem. Biophys. Res. Commun.* **332**, 735–742, ISSN 0006291X, https://doi.org/10.1016/j.bbrc.2005.05.013

147 Miyazaki, M., Jacobson, M.J., Man, W.C., Cohen, P., Asilmaz, E., Friedman, J.M. et al. (2003) Identification and characterization of murine SCD4, a novel heart-specific stearoyl-CoA desaturase isoform regulated by leptin and dietary factors. *J. Biol. Chem.* **278**, 33904–33911, ISSN 00219258, https://doi.org/10.1074/jbc.M304724200

148 Miyazaki, M., Bruggink, S.M. and Ntambi, J.M. (2006) Identification of mouse palmitoyl-coenzyme A Δ9-desaturase. *J. Lipid Res.* **47**, 700–704, ISSN 00222275, https://doi.org/10.1194/jlr.C500025-JLR200

149 Lee, S.H., Dobrzyn, A., Dobrzyn, P., Rahman, S.M., Miyazaki, M. and Ntambi, J.M. (2004) Lack of stearoyl-CoA desaturase 1 upregulates basal thermogenesis but causes hypothermia in a cold environment. *J. Lipid Res.* **45**, 1674–1682, ISSN 00222275, https://doi.org/10.1194/jlr.M400039-JLR200